Published in final edited form as:
Mol Cell Neurosci. 2010 June ; 44(2): 135–153. doi:10.1016/j.mcn.2010.03.003.

Expression by midbrain dopamine neurons of Sema3A and 3F receptors is associated with chemorepulsion *in vitro* but a mild *in vivo* phenotype

Enrique R. Torre[1], **Claire-Anne Gutekunst**[1], and **Robert E Gross**[1,2,*]

[1]Department of Neurosurgery, Emory University School of Medicine, Atlanta, GA

[2]Department of Neurology and Center for Neurodegenerative Diseases, Emory University School of Medicine, Atlanta, GA

Abstract

Here we explore the role of semaphorin 3A and 3F (Sema3A, Sema3F) in the formation of the mesotelencephalic pathway. We show that Sema3A and 3F are expressed in the ventral mesencephalon (VM) of E13.5 rat embryos; the receptors Neuropilin 1 and Neuropilin 2, and coreceptors L1CAM, NrCAM, and Plexins A1 and A3 but not A4 are expressed by VM dopaminergic neurons; these neurons bind Sema3A and 3F *in vitro* which induces collapse of their growth cones and elicits, with different potencies, a repulsive response; and this response is absent in axons from Nrp1 and Nrp2 null embryos. Despite these *in vitro* effects, only very mild anatomical defects were detected in the organization of the mesotelencephalic pathway in embryonic and adult *Nrp1* or *Nrp2* null mice. However, the dopaminergic meso-habenular pathway and catecholaminergic neurons in the parafascicular and paraventricular nuclei of the thalamus were significantly affected in *Nrp2* null mice. These data are consistent with a model whereby Sema3A and 3F, in combination with other guidance molecules, contributes to the navigation of DA axons to their final synaptic targets.

Introduction

In the wiring of the central nervous system (CNS), axons frequently travel long distances following very precise pathways before synapsing with specific target cells, a process that requires a series of structured spatio-temporal signals. While progress has been made in elucidating the signals regulating the formation of several major tracts in the CNS (Garcez et al., 2007; Henion and Schwarting, 2007; Lindwall et al., 2007; Price et al., 2006; Webber and Raz, 2006) the molecular and topographical cues that make possible the formation of the mesotelelencephalic dopaminergic pathways (MTp) is only beginning to be understood.

The MTp is a key component in the basal ganglia thalamo-cortical loop and its disturbance, as a consequence of neurodegenerative diseases like Parkinson's disease (Barzilai et al., 2000; Betarbet et al., 2005; Di Monte, 2003; Hague et al., 2005; Lim and Lim, 2003; Moore et al.,

*To whom correspondence should be addressed: Robert E. Gross, MD, PhD, Department of Neurosurgery, 101 Woodruff Circle, Room 6311, Atlanta, GA 30322, Phone: 404-727-2354, Fax: 404-712-8576, rgross@emory.edu.

Footnote: DA axon guidance by semaphorins

2005) can lead to severe motor and behavioral deficits. The interest in devising restorative therapies for patients suffering from these diseases in part motivates elucidation of the cues involved in the formation of this pathway. The MTp originates in DA neurons in the ventral mesencephalon (VM) whose axons grow rostrally to traverse the diencephalon in a large but well-defined pathway, the medial forebrain bundle (MFB), and reach the telencephalon to synapse on neurons in the nucleus accumbens (mesolimbic pathway) and the striatum (mesostriatal pathway) (Altman and Bayer, 1981; Bayer et al., 1994; Bayer et al., 1995; Voorn et al., 1988). A much smaller group of DA axons originates in rostral cells of the VM, branches off the MFB at the mesencephalon-diencephalon boundary and gives rise to the meso-habenular pathway (MHp) whose axons run along the fasciculus retroflexus and synapse on the lateral habenula (Phillipson and Griffith, 1980; Skagerberg et al., 1984). The MHp has been implicated in the integration of descending output pathways from limbic hypothalamic and striatal forebrain regions and feedback control of the MTp (Gruber et al., 2007; Skagerberg et al., 1984).

During the last decade it has become increasingly clear that bound and soluble signals acting through ligand-receptor signaling can modify growth cone behavior allowing for normal axon pathfinding. Some of these proteins are located on cell surfaces or are part of the extracellular matrix (e.g., laminin, glycans) (Benson et al., 2001; Huber et al., 2003), while others, including semaphorins (Chen et al., 1998a; Chen et al., 1998b; Goshima et al., 2002; Goshima et al., 2000), netrins (Leonardo et al., 1997; MacLennan et al., 1997; Shirasaki et al., 1996; Winberg et al., 1998), ephrins (Barnes et al., 2003; Knoll and Drescher, 2002), and slits (Bagri et al., 2002; Marillat et al., 2002; Niclou et al., 2000) are secreted by neighboring tissue confining the growth of distinct axonal systems to specific pathways. *In vitro* studies indicate that attractive and repulsive signals produced in the VM and diencephalon are indeed involved in the organization of the ventro-mesencephalic DA (vDA) axons into the MTp (Gates et al., 2004; Nakamura et al., 2000b). Netrin1 (Lin et al., 2005; Osborne et al., 2005b) and Sema 3C (Hernandez-Montiel et al., 2008) have been reported to function as attractant signals acting on vDA axons. However, while disturbances of Netrin1 signaling give rise to structural and functional defects of the DA system (Flores et al., 2005), it is not yet clear how deletion of Sema 3C impacts the formation of the MTp.

A few chemorepellent factors have also been implicated in the organization of DA axons. Slits acting through Robo receptors (Brose et al., 1999) expressed by DA neurons (Lin and Isacson, 2006; Lin et al., 2005) may prevent DA axons from crossing the midline (Kawano et al., 2003; Lin et al., 2005) while EphrinB2 and its receptor EphB1 have been implicated in the topographical guidance of the MTp (Yue et al., 1999). Class 3 semaphorins are potent axonal repellents and have been recently implicated in the organization of the MTp. Sema3F, a secreted semaphorin with potent repulsive effects on cortical and sympathetic axons has been shown to repel DA axons (Hernandez-Montiel et al., 2008; Kolk et al., 2009; Yamauchi et al., 2009) and to induce aberrant growth of DA axons in Neuropilin 2 (Nrp2) null mutant mice (Kolk et al., 2009; Yamauchi et al., 2009) while Sema3A, whose mRNA has also been shown to be expressed in the mesencephalon, has been reported to be ineffective on DA axons (Hernandez-Montiel et al., 2008). The receptors for Sema3A and 3F, Neuropilin 1 (Nrp1) and Nrp2, respectively, have been reported to be expressed in the VM and by vDA neurons during development (Hernandez-Montiel et al., 2008; Kolk et al., 2009) and in the adult brain. However, it is not clear whether the plexin coreceptors recruited to the Sema3A/Nrp1 or the Sema3F/Nrp2 complex to transduce the semaphorin signal (Nakamura et al., 2000a; Rohm et al., 2000b; Takahashi et al., 1999; Takahashi and Strittmatter, 2001, Suto, 2005 #61; Yaron et al., 2005), or the cell adhesion molecules L1CAM and NrCAM (Castellani et al., 2000; Castellani et al., 2002; Falk et al., 2005), which are also required for the full manifestation of the repulsive effect of Sema3A and 3F, are expressed by vDA neurons during the organization of the MTp.

Here we show that Sema3A and Sema3F are strongly expressed in the mesencephalon at the time the vDA axons are growing toward the striatum, and that, as previously reported (Hernandez-Montiel et al., 2008; Kolk et al., 2009; Yamauchi et al., 2009), the receptors Nrp1 and Nrp2 are expressed by vDA neurons and their axons enabling them to bind to both Sema3A and 3F. We show that the transducers PlexinA1 and A3, but not A4, and the coreceptors L1CAM and NrCAM, are expressed by vDA neurons. In line with these observations, in *in vitro* experiments Sema3A and 3F induced with different potencies the collapse of DA growth cones and a significant repulsive response on DA axons. However, the potency with which these semaphorins modify the response of the DA axon *in vitro* contrasted with the finding of very mild defects in the gross anatomical organization of the VM DA system as well as the lack of a behavioral phenotype in *Nrp1* and *Nrp2* knockout mice. The results suggest that Sema3A and 3F signals play a role in the organization of the DA MTp, but that their absence is largely compensated leaving the nigrostriatal and meso-limbic synaptic organization largely unimpaired.

Results

Sema3A and Sema3F are expressed in the VM region of the mesencephalon

We first explored the expression pattern of Sema3A and 3F during the development of the MTp. In parasagittal sections of E13.5 rat embryos the staining for Sema3A in the VM defined an increasing gradient that extended from the floor of the ventricle up to the pial surface (Fig. 1A). Most of the tyrosine hydroxylase immunostained (TH^+) neurons were localized in the more densely Sema3A stained areas of the VM. Caudal to the VM the gradient is replaced by a strong staining that remains confined to the ventral portion of the rhombencephalon and spinal cord. Some sections showed a dense track of axons originating in the rostral mesencephalon, presumably the medial longitudinal fasciculus (Belanger et al., 1997;Mastick and Easter Jr, 1996), that was strongly stained for Sema3A.

Sema3F staining was confined to the ventral aspect of the spinal cord and rhombencephalon, extending dorsally in the VM and hindbrain. In medial regions of the VM the distribution of the Sema3F signal is stronger than in the rostral rhombencephalon and dorsal VM (Fig 1B). In addition, a rostrally-decreasing gradient of the Sema3F signal that coincided with that previously reported for its mRNA (Funato et al., 2000;Giger et al., 2000;Kolk et al., 2009;Melendez-Herrera and Varela-Echavarria, 2006) accentuates a caging pattern that appears to surround the vDA neurons (Fig. 1B, D). This pattern seems to dissipate in more lateral sections (Fig. 1C) where the staining becomes evenly distributed.

The receptors for Sema3A and Sema3F are expressed by vDA neurons both in vivo and in vitro

We used immunochemical approaches to evaluate whether vDA neurons, both in tissue and in dissociated VM cultures, expressed the receptors for Sema3A and Sema3F. In E13.5 rat embryos, the signal for the Sema3A receptor, Nrp1, was weak and detected in some vDA neurons and a larger number of non-DA neurons (Fig. 2). The Sema3A/Nrp1 complex recruits plexins to transduce the semaphorin signal. Of the possible transducers, PlexinA1 showed a weak signal that, like the Nrp1 signal, was only associated with few vDA neurons. Both proteins were immunodetected along the MFB in small patches, sometimes associated with axonal varicosities, and frequently co-localizing with TH^+ axons running on the dorsal aspect of the MFB (Fig. 2). Surprisingly, PlexinA4 - the obligatory transducer for Sema3A at least in sensory and sympathetic neurons (Suto et al., 2005;Yaron et al., 2005) - was not expressed by vDA neurons but by cells that extended radially from the ventral surface toward the ventricle. Double staining with Nestin identified these cells as radial glia (Park et al., 2009;Wei et al., 2002) (Fig. 2). Strong staining of hippocampal and cortical neurons in the same section (Gutekunst et al.,

submitted), two regions whose axons are strongly repelled by Sema3A (Chen et al., 1997), ruled out a technical artifact as the cause for the lack of staining of vDA neurons (data not shown).

In addition to plexins, the full effect of Sema3A in several neuronal systems requires the association with L1CAM (Castellani, 2002; Castellani et al., 2000; Castellani et al., 2002; Wright et al., 2007). Since it has been reported that L1CAM can affect the distribution (Demyanenko et al., 2001) and survival of vDA neurons (Hulley et al., 1998) we also investigated whether L1CAM was expressed in the VM in general, and by vDA neurons in particular. Confocal microscopic analysis revealed that at E13.5 the L1CAM signal co-localized with a small fraction of the TH-expressing neurons in the VM (Fig. 2) that was consistent with what we found for Nrp1 and PlexinA1. As shown in Fig. 2, the signal for L1CAM in the VM was largely associated with the extracellular space surrounding vDA neurons and the axons emerging from VM and running along the MFB.

Cultured vDA neurons expressed the same complement of receptors found *in vivo* (Fig. 3A). Nrp1 and PlexinA1 co-localized in TH^+ neurons but, as seen in brain sections, the PlexinA1 signal was light with a somewhat more diffuse distribution than that of Nrp1. The staining of Nrp1 and PlexinA1 was characterized by a fine punctate pattern that generally colocalized in cell bodies, axons, and particularly in growth cones of TH^+ neurons (Fig. 3A). As in brain sections, PlexinA4 antibodies did not stain cultured vDA neurons. In contrast, L1CAM was strongly expressed by vDA neurons in culture although a fraction of the TH^+ axons remained unstained for this antigen (Fig. 3A).

We next investigated whether the proteins that comprise the receptor complex for Sema3F were expressed by vDA neurons. E13.5 embryonic rat brain sections and cultures from dissociated E14 VM were double-stained for Nrp2, PlexinA3 or NrCAM, and TH. At E13.5 both the Sema3F receptor Nrp2 and the signal transducer PlexinA3 were expressed by TH^+ and non-TH immunoreactive (TH^-) cells in the VM (Fig. 4). Staining for Nrp2 was particularly intense and co-localized with a large number of TH^+ neurons and extended into axons in the MFB. PlexinA3 staining was weaker and appeared in a punctate pattern within many vDA neurons and also extended into TH^+ axons along the MFB (Fig. 4). Finally, we examined the expression of NrCAM -an immunoglobulin superfamily adhesion molecule of the L1 subfamily- that has been reported to associate with Nrp2 and be a component of a receptor complex for Sema3B and Sema3F (Falk et al., 2005). In E13.5 rat brain embryos NrCAM immunoreactivity was detectable in the VM. However, the signal was predominantly associated with the extracellular matrix, surrounding DA and non-DA cells and underlying TH^+ axons that extend along the MFB. Some TH^+ neurons in the VM and axons along the MFB were also immunoreactive for NrCAM (Fig. 4).

Nrp2, PlexinA3 and NrCAM labeled dissociated vDA neurons in culture as well. The staining was generally distributed along axons and growth cones (Fig. 3B). Whereas PlexinA3 was more enriched in TH^+ neurons, Nrp2 and NrCAM were expressed by both TH^+ and TH^- neurons, and most axons were NrCAM immunoreactive.

Sema3A and Sema3F bind to dissociated DA neurons in culture, induce the collapse of DA-growth cones and repel DA axons in vitro

The expression of the receptors Nrp1 and Nrp2, their signal transducers PlexinA1 and A3 and coreceptors L1CAM and NrCAM by vDA neurons suggested Sema3A and 3F may be bound by functional receptor complexes that could then elicit a repulsive response in vDA axons. Cultures of VM dissociated neurons were affinity labeled using His/flag-tagged Sema3A or myc-tagged Sema3F conditioned media and the binding of the guidance molecules to vDA neurons was verified by immunocytochemistry. Sema3A conditioned media labeled both vDA

and non-DA neurons producing a weak punctate pattern sparsely associated with axons and growth cones (Fig. 5A2). In contrast, Sema3F binding produced a more selective and intense labeling of TH^+ neurons (Fig. 5A4). Sema3F puncta were densely distributed along the shaft of the axon and the surface of growth cones resembling the distribution pattern of Nrp2. The specificity of the Sema3A and 3F labeling is further supported by the absence of any specific labeling following the incubation of the cells in media conditioned by normal untransfected 293T cells (Fig. 5A2 and 4).

Next, we evaluated whether these associations affect the growth cone dynamics and induce a repulsive response on TH^+ axons. Growth cone collapse assays were conducted on 5-day-old VM aggregates growing on PLL/laminin-treated coverglasses. Axons extending from the aggregates were exposed to media conditioned by either un-transfected (control) or stably Sema3A or 3F-transfected 293T cells (Puschel et al., 1995). The growth cone area of TH^+ axons was reduced 27% when treated with Sema3A (Fig. 5B1 and 2). This change reflected an increase in medium size and fully collapsed growth cones whereas the number of growth cones with large area appeared unaffected. The area of fully collapsed TH^+ axons (a tapered axonal terminal without spread lamellipodia) when measured within 10 μm of its tip ranged from 7 to 25 μm^2. The number of fully collapsed axons, although increased four-fold with respect to controls, represented about 10% of the growth cone population (Figure 5B3b). In contrast, a larger proportion of TH^+ growth cones collapsed when exposed to Sema3F. This was reflected by a decrease of more than 60% in the growth cone area (Fig. 5B2) where the number of large growth cones was dramatically diminished and more than 45% percent of the growth cone areas were compatible with fully collapsed axons (Fig. 5B3b). The collapsing effect of Sema3F on TH^+ growth cones was abrogated by pre-treatment with anti-Nrp2 antibodies. Since pre-treatment with antibodies against Nrp1 did not affect the response to Sema3F (Fig. 5B2) we concluded that the effect of Sema3F on DA growth cones is solely mediated by the Nrp2 receptor.

To verify if the collapse of vDA growth cones correlated with a repulsive response we set up co-cultures where VM explants, dissected from E14 rat embryos, were embedded with untransfected (control) or stably Sema3A/3F-transfected 293T cells aggregates in a mixture of collagen/Matrigel as described previously (Puschel et al., 1995). Co-cultures were maintained for 2-3 days, fixed and double-labeled for tubulin and TH to evaluate the response of both DA and non-DA axons. The effectiveness of Sema-secreting cell aggregates in repelling axons was established in parallel control co-cultures using dorsal root ganglia or hippocampal tissue explants whose axons are known to be repelled by Sema3A whereas they are unresponsive to or strongly repelled by Sema3F, respectively (Chen et al., 1997; Dontchev and Letourneau, 2002; Fu et al., 2000; Kawasaki et al., 2002; Masuda et al., 2003; Scarlato et al., 2003; Suto et al., 2003; Yaron et al., 2005). As expected, Sema3F-secreting aggregates produced a strong repulsive effect on TH^+ and TH^- axons extending from VM explants (Fig. 6A and B). Although in most experiments some TH^+ as well as TH^- axons escaped the repulsive action of Sema3F, in general the repulsive effect of Sema3F consistently induced P/D ratios below 50 in about 80% of the VM explants and 50% of the brain stem explants. However, this response was significantly weaker than that exerted on hippocampal axons (VM P/D = 38.64 ± 4.86 vs. Hc P/D = 23.3 ± 3.9. $p<0.01$) possibly due to a less robust expression of Nrp2/PlexinA3 receptors in the VM. The repulsive effect induced by Sema3F was significantly reduced or practically eliminated in co-cultures set up with VM explants dissected from E14 *Nrp2*$^{+/-}$ and *Nrp2*$^{-/-}$ mice embryos, respectively. Only 37% of the *Nrp2*$^{+/-}$ and practically none of the *Nrp2*$^{-/-}$ co-cultures were repelled by Sema3F (Fig. 6D), further supporting the specificity of the repulsive response of vDA axons to Sema3F and the direct involvement of Nrp2 in eliciting this response.

In contrast, the response of TH^+ axons to Sema3A was weaker and inconsistent. Measured by the P/D ratios this response was undistinguishable from controls (Sema3A P/D: 90.7 ± 3.5;

293T P/D: 97.7 ± 2.5; Fig. 7B) where TH^+ axons were frequently seen growing on and/or around the Sema3A cell aggregates. A small but significant repulsive effect of Sema3A was detected on non-DA axons from brain stem co-cultures that was consistent with the localization of the Sema3A receptor in a larger number of TH^- cells in this region. The possibility that insufficient levels or quality of the secreted Sema3A was responsible for the poor response of VM or brain stem axons was ruled out by controls indicating that axons from hippocampal and DRG explants were strongly and consistently repelled by Sema3A secreting cells (90 to 100 % of the co-cultures produced P/D ratios smaller than 30) (Fig. 7B). It was intriguing that despite this apparent lack of effect of Sema3A upon TH^+ positive axons we frequently observed co-cultures strongly repelled or attracted by Sema3A secreting cells (Fig. 7A). Whereas the distribution of the individual P/D ratios for 293T or Sema3F/VM co-cultures fall into well differentiated clusters, those for Sema3A overlapped with both groups (Fig. 7D). We reasoned that if the population of Sema3A-responsive DA neurons is small, only the explants containing a large percentage of them might exhibit a clear repulsive response while the response might proceed unnoticed in explants in which the fraction is smaller. Thus, we decided to re-evaluate these results by scoring the response of each co-culture by its P/D ratio. Cultures with P/D ratios that were <1 standard deviation (S.D.) below the control mean were scored as repelled while those that were >1 S.D. above the control mean were scored as attracted. P/D ratios falling between these limits defined unresponsive cultures. This approach revealed that TH^+ axons from one third of the cultures were significantly repelled by Sema3A while the attractive effect was not statistically different from that exerted by untransfected 293T cell aggregates (Fig. 7E). Although DA axons can sometimes be repelled by control 293T-cell aggregates the incidence of these responses was significantly larger and stronger when facing Sema3A secreting cells (Repulsion 293T: 14.4±5.2; Sema3A: 34.75±5.7, $p < 0.02$; Fig. 7E). Similar to Sema3F, the response elicited by Sema3A on DA axons is significantly weaker than that elicited on hippocampal axons. Nevertheless, the disappearance of this subpopulation of Sema3A responsive DA neurons in co-cultures using VM explants from conditionally deleted mice (*TH-Cre*$^+$;*Nrp1*$^{c/c}$) further supports their existence (Fig. 7D and E).

Embryonic and adult Nrp2 knockout mice and conditional Nrp1 knockout mice manifest mild defects of the MTp

Ventro-mesencephalic DA neurons in the ventral tegmental area (VTA) and substantia nigra pars compacta (SNc) express the receptor complexes necessary for the binding and transduction of Sema3A and 3F signals. *In vitro* studies showed that, indeed, axons from these cells could be repelled by both semaphorins. Thus, we postulated that the absence of the binding receptors Nrp1 or Nrp2 might lead to anatomical defects in the organization of the MTp. This possibility was investigated in E12, E14, E16 embryos and adult *Nrp2*$^{-/-}$ or *TH-Cre*$^+$;*Nrp1*$^{c/c}$ (data not shown) mutant mice and their wild type littermate controls. DA neurons and their axonal projections were visualized in coronal and parasagittal brain sections by TH immunocytochemistry. Despite the repulsive effects of Sema3A and 3F in the *in vitro* studies described above, no clear differences were observed in either mutant in the number of TH^+ neurons, or their position in VTA or SNc of embryonic or adult mice (Figs. 8 and 9).

The TH^+ fibers in the MFB as well as the striatal terminal field exhibited an identical appearance in *Nrp1* mutant as compared to wild type mice at all ages studied (data not shown). The lack of an obvious anatomical phenotype in the MTp of the *TH-Cre*$^+$;*Nrp1*$^{c/c}$ mutant mice is not surprising in view of the small number of Nrp1 expressing DA neurons as well as the weak response to Sema3A by vDA axons. Thus, if the signaling mediated by Nrp1 is not compensated the presence of aberrant growing axons might be masked by the more abundant population of normal DA axons.

Despite the strong and extensive response of DA axons to Sema3F we observed a very mild anatomical phenotype in *Nrp2*$^{-/-}$ mutant mice (Fig. 8), in contrast to the severe defects of several major central axonal tracts including the anterior commissure and the fasciculus retroflexus (Chen et al., 2000;Giger et al., 2000). It was recently reported that in *Nrp2*$^{lacZ/lacZ}$ knockout mice (Yamauchi et al., 2009), and also in *Nrp2*$^{-/-}$ (used in our studies), *Sema3F*$^{-/-}$ and *Nrp2*$^{-/-}$;*TH-Cre* conditional knockout mouse strains (Kolk et al., 2009), DA axons originating in the VM became defasciculated and spread dorsally, while a subset of them grew aberrantly into the rostral hindbrain. In our studies, however, these anatomical phenotypes were much less striking or absent. We indeed observed very mild dorsal expansion in the area occupied by TH$^+$ axons in the MFB, confined to a region extending rostral to the VM and descending into the hypothalamus. However, the combined measurements of the MFB area (Fig. 8B) and width (data not shown), both laterally and along the track, were not significantly different statistically between *Nrp2*$^{-/-}$ and control littermates. The most dramatic of these phenotypes, the growth of TH$^+$ neurites toward the hindbrain was seen in only one out of 16 *Nrp2*$^{-/-}$ mice examined, despite our meticulous replication of the anatomical and immunological techniques described by Yamauchi et al. (Yamauchi et al., 2009). In this case not only neurites but also TH$^+$ neurons were seen extending caudally toward the frontal rhombencephalon (Fig. 8B). Finally, it was reported that TH$^+$ fibers in the MFB become dramatically defasciculated in *Nrp2* and *Sema3F* mutant mice (Kolk et al., 2009). However, we could not detect this phenotype in E12 to E16 *Nrp2*$^{-/-}$ mice. Using confocal as well as conventional light and fluorescent microscopy we found that TH$^+$ fibers descending into the hypothalamus of both E13-14 *Nrp2*$^{-/-}$ and wild type mice brains were mildly fasciculated (Fig. 8 and see also Fig. 2 and 4), a pattern that persisted into E16 brains. In brains from both *Nrp2*$^{-/-}$ and wild type littermates, TH$^+$ fibers run closer together through the hypothalamus toward the internal capsule. The organization of these fibers into fascicles becomes apparent at E14 and is truly organized as discrete bundles by E16.

In contrast, we observed the DA mesohabenular track to be in disarray in the *Nrp2*$^{-/-}$ knockout mice (Fig. 8C). This subset of DA axons originating in the rostral VTA branch off the MFB and ascend along the fasciculus retroflexus to synapse in the lateral habenula (Phillipson and Griffith, 1980;Skagerberg et al., 1984). As reported previously, the fasciculus retroflexus - an axonal track originating in cells of the medial habenula that descends to the interpeduncular nucleus under the tight control of Sema3F signaling - is severely affected in Sema3F (Sahay et al., 2003) and *Nrp2* knockout mice (Giger et al., 2000;Yamauchi et al., 2009). In our *Nrp2*$^{-/-}$ mice the fasciculus retroflexus loses its compactness and definition and although it still can be detected in parasagittal brain sections (Fig. 8C) it is hardly visible in coronal sections (Fig. 8A and 9). TH-immunostaining revealed that in *Nrp2*$^{-/-}$ E-16 embryos the number of DA axons in the mesohabenular pathway is significantly reduced and the remaining ones appear stunted and varicose (Fig. 8C). This defect persists in the adult *Nrp2*$^{-/-}$ mutant mice since a perceptible reduction in the number of DA fibers could still be detected in the lateral habenula. Unfortunately, the low number of DA axons reaching this nucleus makes a more accurate quantitation difficult.

In adult brains of the *Nrp2*$^{-/-}$ mutant mice we found several defects in the number and distribution of TH$^+$ non-DA neurons and fibers in the medial region of the nucleus parafascicularis (PF). A small subset of non-DA TH$^+$ neurons normally detected bilaterally close to the midline in the paraventricular nucleus of the thalamus of wild type mice appeared significantly denser and lateralized in the *Nrp2*$^{-/-}$ mice (Fig. 9B 1 and 1′). Similarly, a few non-DA TH$^+$ neurons stained along the medial edge of the fasciculus retroflexus and their axons extend medially and may cross to the contralateral side. Coinciding with the distribution of the TH mRNA depicted in the Allen Mouse Brain Atlas (Lein et al., 2007) most of these cells are distributed ventrally in the thalamus. In contrast, in the *Nrp2*$^{-/-}$ mutant mice the number of these cells and their fibers increases significantly and extends more dorsally (Fig. 9B 2 and 2′).

Axons from other non-DA TH^+ neurons like those originating in the locus coeruleus showed no significant differences with the pattern found in wild type animals.

The silencing of Sema3A or Sema3F signaling does not elicit a behavioral phenotype

The strong repulsive effects elicited by Sema3A and 3F *in vitro* encouraged us to examine the basic components of motor behavior in the adult *Nrp2*$^{-/-}$ or *TH-Cre*$^{+}$;*Nrp1*$^{c/c}$ mutant mice and their littermate controls. Consistent with the lack of an anatomical phenotype, the adult *TH-Cre*$^{+}$;*Nrp1*$^{c/c}$ mutant mice showed no behavioral differences with control littermates when locomotion, rearing, total distances and stereotypic activities (head movements, grooming, etc.) were measured (data not shown). In contrast, the *Nrp2*$^{-/-}$ mutant mice exhibited a reduced motor activity such that the measured distance traveled in the 30 min test amounted to less than 50% of the values measured in wild type animals (Fig. 9C). We also used a biased conditioned place preference (CPP) test to evaluate the *Nrp2*$^{-/-}$ mutant mice. This approach is commonly used to measure the rewarding or aversive effects of drugs and requires an intact mesolimbic DA system (Bals-Kubik et al., 1993;Gong et al., 2007;Tzschentke, 1998). Thus, changes in the wiring of the striatum by defects in the MTp induced by silencing Sema3F might modify the response in the CPP test. In these studies the preference elicited by cocaine in the *Nrp2*$^{-/-}$ mutant mice was undistinguishable from wild type littermates (Fig. 9D).

Discussion

At E13-14 the class 3 semaphorins Sema3A and Sema3F are expressed in the mesencephalon in the territory where DA neurons will migrate, differentiate and mature. We used *in situ* and *in vitro* techniques to examine the possible functional roles of Sema3A and 3F during the early stages of the formation of the MTp, finding the following. First, despite reports indicating low levels of Sema3A mRNA expression in the midbrain (Melendez-Herrera and Varela-Echavarria, 2006), Sema3A was strongly expressed in this region producing a pattern resembling an increasing dorso-ventral gradient. At this same embryonic stage Sema3F was also strongly expressed, paralleling the distribution of its mRNA at E13 (Funato et al., 2000; Hernandez-Montiel et al., 2008; Kolk et al., 2009; Melendez-Herrera and Varela-Echavarria, 2006), defining a caudal to rostral decreasing gradient that surrounded the population of TH^+ neurons. Second, at E13/14, as previously reported (Hernandez-Montiel et al., 2008; Kolk et al., 2009), a subpopulation of vDA neurons expressed the Nrp1 receptor. In addition, the coreceptor L1CAM and the transducers PlexinA1 and A3, but not A4 were expressed by vDA neurons. In contrast, a larger number of vDA neurons expressed proteins that would make possible the formation of a Sema3F receptor complex, both *in vivo* and *in vitro*, including Nrp2 (Funato et al., 2000; Hernandez-Montiel et al., 2008; Kolk et al., 2009; Yamauchi et al., 2009) and this work), PlexinA3 and NrCAM. Third, we found that in dissociated cultures Sema3A and 3F bind to vDA neurons inducing, with different potencies, the collapse of TH^+ growth cones, and eliciting a strong repulsive effect on vDA axons. The existence of Sema3A and 3F responsive vDA neurons was further supported by the loss of the repulsive response in cultures from *TH-Cre*$^{+}$;*Nrp1*$^{c/c}$ or *Nrp2*$^{-/-}$ mutant mice. Finally, despite the susceptibility of vDA axons to be repelled by Sema3A and 3F *in vitro* very mild changes in the gross anatomical organization of the MTp were detected in embryonic or adult brains of *TH-Cre*$^{+}$;*Nrp1*$^{c/c}$ or *Nrp2*$^{-/-}$ mutant mice.

The role of Sema3A in the formation of the meso-telencephalic DA pathway

At E13.5 Sema3A has a very distinctive expression pattern in the VM, concentrated ventrally and gradually decreasing toward the aqueduct. In addition, Sema3A is strongly expressed by axons, presumably belonging to the medial longitudinal fasciculus (Belanger et al., 1997; Mastick and Easter Jr, 1996), that by its organization in the anterocaudal axis might play a role in informing Nrp1 expressing TH^+ axons in the VM. At this stage most DA neurons have

already reached the ventral surface of the mesencephalon, concentrating at both sides of the midline (Kawano et al., 1995), are producing TH and DA, and their axons are growing toward the striatum (Altman and Bayer, 1981; Perrone-Capano and Di Porzio, 2000; Voorn et al., 1988). A recent report showed that these neurons express Nrp1, Nrp2, both or neither of these receptors suggesting that in the VM there are DA neurons with distinct capabilities to respond to Sema3A and/or 3F (Hernandez-Montiel et al., 2008). The finding of PlexinA1 and A3 in TH^+ axons along the MFB suggests that those axons might still respond to Sema3A, and consistent with this we found that the Sema3A signal could generate a repulsive response in a subpopulation of TH^+ neurons *in vitro*, which is absent in explants from the *TH-Cre*$^+$;*Nrp1*$^{c/c}$ mouse. These results contrast with a previous report (Hernandez-Montiel et al., 2008) where the effect of Sema3A on DA axons was defined as trophic rather than tropic. Axons were neither repelled nor attracted but the number of axons growing out of the explants increased when exposed to Sema3A expressing cell aggregates. In about one third of our VM co-cultures more and longer axons appeared to grow toward the Sema3A-expressing cell aggregates, resulting in P/D ratios that were sometimes equivalent to those of an attractive response. When these cultures were scored as “attracted”, however, the group was not significantly different from those attracted to untransfected 293T cells suggesting that some intrinsic factor produced by 293T cells might work as a weak attractant to the DA axon, an activity that might be enhanced in co-cultures using *TH-Cre*$^+$;*Nrp1*$^{c/c}$ VM cells in which the repulsive effect of Nrp1 is deleted in DA neurons. Thus, it is possible that the more stringent conditions of the repulsion paradigm used by Hernandez-Montiel et al. (Hernandez-Montiel et al., 2008) made it harder for the detection of this weak response in a low number of responsive cells.

Recent reports showed that the Sema3A receptor requires the association of Nrp1 with PlexinA4 or, to a much lesser extent, PlexinA3 to serve as signal transducers (Cheng et al., 2001; Suto et al., 2005; Yaron et al., 2005). Therefore, it was surprising to find that the PlexinA4 signal was absent in vDA neurons, but rather was associated with TH^- cells, many of them identified as radial glia by their morphology, organization and co-localization with Nestin (Dahlstrand et al., 1995; Park et al., 2009). In contrast, both PlexinA3 and PlexinA1 were expressed by TH^+ neurons *in vivo* and *in vitro*. PlexinA1, a protein that has been repeatedly shown to associate with Nrp1 and to transduce the Sema3A signal when co-expressed *in vitro* (Bachelder et al., 2003; Catalano et al., 2004; Deo et al., 2004; Mitsui et al., 2002; Rohm et al., 2000a; Takahashi et al., 1999; Takahashi and Strittmatter, 2001), was detected in many TH^+ and TH^- cells in the VM, along numerous TH^+ fibers of the dorsal MFB and in cultures of VM neurons. Thus, PlexinA1 and/or A3 might be recruited to the Sema3A-Nrp1/L1CAM complex and be capable of propagation of the Sema3A signal. Our finding of Nrp1 and PlexinA1 co-localizing in TH^+ neurons in culture (Fig. 3A) supports the possibility that this association can occur. The formation of this particular receptor complex may explain why the repulsive response elicited by Sema3A was weaker than that elicited by Sema3F and much weaker and less reliable than that evoked on hippocampal explants.

The Sema3A receptor also requires L1CAM, associating in cis or cis/trans, which contributes to or changes the Sema3A response, respectively (Castellani et al., 2000; Castellani et al., 2002). We found L1CAM largely associated with the extracellular matrix and TH^- fibers while few TH^+ neurons were stained in the VM, a view that agrees with previous reports (Demyanenko et al., 2001; Ohyama et al., 1998). In contrast, numerous TH^+ fibers in the MFB, and a large fraction of TH^+ axons in VM cultures, stained for L1CAM suggesting that it is likely that more vDA cells express this protein, but it becomes easier to detect it in axons where it appears to be enriched. Reports indicating that L1CAM (Munakata et al., 2003) and its mRNA (Horinouchi et al., 2005) are expressed by numerous presumably DA cells in the VTA and SNc of the adult mouse would support this possibility.

The low number of vDA neurons capable of responding to Sema3A as well as the weak repulsive response elicited by it suggests that Sema3A might not be a decisive player in the initial steering of DA axons in the MTp, consistent with the lack of significant differences in the gross anatomical organization of the MTp as well as the absence of a behavioral phenotype in the Nrp1 conditional knockout mutant mice. However, even in the absence of a robust anatomical phenotype, it is possible that Sema3A is involved in other more nuanced processes such as pre-target axon sorting (Imai et al., 2009), thus contributing to establishing the topographical organization of the terminal fields in the accumbens and caudate/putamen (Haber, 2003; Joel and Weiner, 2000). Another possibility, based on the increasing distribution of Sema3A from the aqueduct to the ventral midbrain, is that it may be involved in the migration of newly formed DA neurons, which originate in the aqueduct and follow radial glia to reach the ventral mesencephalon (Shults et al., 1990). Sema3A was only recently proposed to be a likely player in cell migration during development (Bagri and Tessier-Lavigne, 2002; Eickholt et al., 1999; Kurschat et al., 2006; Osborne et al., 2005a; Spassky et al., 2002; Tamamaki et al., 2003; Tsai and Miller, 2002) and it has been recently shown to be a key player in the radial migration of cortical neurons (Chen et al., 2008). Thus, our observations suggest the possibility that an increasing expression of Sema3A in the ventral mesencephalon may signal DA neurons to end their ventral migration.

Sema3F is a potent repellant of vDA axons

In contrast to the limited effects of Sema3A on DA axons, Sema3F unequivocally elicited a strong collapsing effect on DA growth cones and repulsive response of DA axons *in vitro*, suggesting that it may contribute to the rostral orientation of the DA axons in the VM. However, the response elicited by Sema3F on DA axons was still significantly weaker than hippocampal axons, possibly related to the expression level of receptor complexes or other downstream signaling components. Specifically, PlexinA3 may need the co-expression of PlexinA4 to mediate the full effect of Sema3F (Yaron et al., 2005), and since vDA neurons do not express PlexinA4 the propagation of the Sema3F signal might be accomplished solely through PlexinA3 and/or PlexinA1 (Cheng et al., 2001). That other plexins might be used in the Sema3F receptor complex has been suggested by findings showing that a subset of the abnormalities detected in both Sema3F and Nrp2 null mutant mice (Catalano et al., 1998; Chen et al., 2000; Giger et al., 2000; Sahay et al., 2003) are not manifested in the PlexinA3 null mice (Yaron et al., 2005). An alternative explanation is that, similar to Sema3A, Sema3F may be differentially processed by furin enzymes (Adams et al., 1997) in the VM region thereby attenuating its potency.

Decreased activity of Sema3F in vDA neurons may account for our failure to detect a striking *in vivo* phenotype. Most of the studies using Sema3F null mice or knockouts for its receptor components (e.g. Nrp2, PlexinA3) (Catalano et al., 1998; Chen et al., 2000; Giger et al., 2000; Sahay et al., 2003), A4 (Yaron et al., 2005), and NrCAM (Falk et al., 2005) have not reported alterations in the MTp, suggesting that the deficits, if any, are subtle. However, two recent reports showed that elimination of Nrp2 (Kolk et al., 2009; Yamauchi et al., 2009) or Sema3F (Kolk et al., 2009) led to an apparent dorsal expansion of the MFB accompanied by the loss of fasciculation of the ascending TH^+ fibers. In addition, the aberrant growth of a significant number of DA fibers that extended caudally toward the rhombencephalon was described in the *Sema3F*$^{-/-}$ as well as the three *Nrp2* knockout strains (Kolk et al., 2009; Yamauchi et al., 2009). These observations are in partial disagreement with the results presented here. While the MFB seemed to run as a tighter bundle in wild type as compared to *Nrp2*$^{-/-}$ mice, where a dorsal spread of TH^+ fibers - particularly in the region rostral to the substantia nigra and descending into the hypothalamus is apparent, measurements of both the width of the MFB and the mean area occupied by TH^+ fibers in several contiguous sagittal sections failed to produce statistically significant differences from wild type (although the

sample size was small accounting for the failed statistical test, this is nevertheless an indication of the subtlety of the finding). Regarding the fasciculation of TH^+ fibers: light, fluorescent and confocal microscopy presented a similar picture in wild type and *Nrp2*$^{-/-}$ brains that contrasted with that described by Kolk et al. (Kolk et al., 2009). In our studies of E12 to E14 embryos, TH^+ axons, particularly in the region rostral to the VM and descending into the hypothalamus, ran individually or in small bundles. In the hypothalamus/thalamus region TH^+ axons run close together and mild fasciculation began to appear by E14 becoming striking by E16 (see Fig. 8A,B). Although this disagreement might be attributed to technical variables we cannot completely discard subtle differences in the animal strains due to housing or breeding manipulations (2009; Gerlai, 1996; Phillips et al., 1999; Steward and Trimmer, 1997). Thus, despite the role that Nrp2 may play in axonal fasciculation (Cloutier et al., 2002) its absence in the *Nrp2*$^{-/-}$ mice did not dramatically alter the organization of TH^+ fibers in the MFB. Finally, the aberrant growth of DA fibers towards the rhombencephalon (Kolk et al., 2009; Yamauchi et al., 2009) was only detected it in one out of sixteen embryos examined between E12 and E16. However, despite the low incidence of this phenotype in the *Nrp2*$^{-/-}$ mouse it appeared to be more dramatic than that seen in the *Nrp2*$^{lacZ/lacZ}$ knockout mouse since it involved not only the fibers but also TH^+ neurons (see Fig.8). That our anatomical results likely reflect a true phenotypic difference rather than a technical artifact is supported by several lines of reasoning. First, we were able to observe the mutant phenotype, albeit in only one animal, ruling out technical immunohistochemical issues. Second, the possibility that the results were due to inaccurate genotyping is unlikely since (a) the animals were genotyped twice, and (b) as discussed further below, other phenotypic abnormalities were detected involving TH^+ axons.

In contrast to the mild phenotype in the MTp, we detected a significant deficit in a minor DA track originating in the VTA and branching off the MFB, the mesohabenular pathway, that ascends through the fasciculus retroflexus to innervate the lateral habenula (Gruber et al., 2007; Phillipson and Griffith, 1980; Skagerberg et al., 1984). This abnormality might be secondary to the severe defects in the fasciculus retroflexus present in these mice, or to the lack of Sema3F signaling impinging on the DA axon. Indeed, TH^+ axons in the MHp were reduced in number and length while their varicose appearance suggested an unhealthy state. Given the scarcity of DA axons ascending in the MHp it was difficult to determine the degree of alteration along the track, but TH-staining in the lateral habenula of adult mice suggested that the number of DA axons reaching their target was reduced. In addition, non-DA TH^+ neurons were abnormally distributed in the paraventricular nucleus of the thalamus. More strikingly, in the nucleus parafascicularis and the periventricular gray area a larger number of non-DA TH^+ neurons and neurites expanded into a territory usually not occupied by them. Sema3F is a potent anti-tumor factor that can act not only through Nrp2 but also Nrp1, and it has been shown that Sema3F can inhibit cell adhesion and migration in several tumor cell lines (Nasarre et al., 2003; Potiron et al., 2007; Shimizu et al., 2008) and also in neurons (Tamamaki et al., 2003). Thus our finding suggests that the silencing of Sema3F in those areas might have eliminated an inhibitory signal that prevented non-DA TH^+ cells from invading the region. This is an interesting observation that might directly link Sema3F to the migration of some catecholaminergic neuron subpopulations.

Implications for development of the meso-telenecephalic DA pathway

Although the precise molecular determinants that guide DA axonal projections from the ventral midbrain to the striatum and elsewhere are still poorly understood, several axon guidance molecules have been implicated, including EphrinB1 (Yue et al., 1999), Netrin-1 (Bagri et al., 2002; Flores et al., 2005; Lin and Isacson, 2006; Lin et al., 2005; Vitalis et al., 2000). Based on the absence of Sema3A- and Slit2-expressing (Kawano et al., 2003) ventricular neuroepithelium in Nkx2.1 – deficient mice, it was proposed that Sema3A and/or Slit repel developing ventral midbrain DA neurons thus preventing them from crossing the midline.

However, the small number of cells affected by Sema3A in the VM as well as the mild repulsive response elicited by Sema3A makes it an unlikely candidate for playing a critical role in preventing DA axons from crossing the midline. Our anatomical analysis in adult *TH-Cre*$^{+}$;*Nrp1*$^{c/c}$ mice further supports this conclusion.

Our results point to Sema3F as a more likely candidate to be one of the active repulsive signals emanating from both the caudal midbrain (Gates et al., 2004) and the dorsal mesencephalon (Nakamura et al., 2000b) that lead to the rostral orientation of the TH positive fibers exiting the VM. The expression pattern of Sema3F in fact suggests a significant role in channeling the dopaminergic fibers towards the telencephalon. Moreover, the combined action of Sema3F in the VM and the hindbrain (Funato et al., 2000) and Slit1/2 in the ventricular zone and hypothalamus may later contribute to the packaging of the DA axons within the MFB in its passage to the striatum. The presence of other guidance molecules in the VM as well as other receptors that can be recruited into the Sema3F receptor complex may explain that the silencing of the Sema3F signal can be compensated leading to the absence of a stronger anatomical phenotype. The lack of an *in vivo* phenotype despite strong effects *in vitro* has been repeatedly reported for class 3 semaphorins (Catalano et al., 1998; Kitsukawa et al., 1997; Taniguchi et al., 1997). Our data suggests that Sema3A and 3F are part of the array of attractive and repulsive signals steering the DA axon on its path toward the striatum and mesolimbic cortex. As visualized by Tessier-Lavigne and Goodman (Tessier-Lavigne and Goodman, 1996) the requirement of multiple cues may be critical to ensure the completion and accurate targeting of a developing axonal tract, and because of that complexity the absence of a stronger anatomical phenotype in the *Nrp2*$^{-/-}$ mice, although surprising, fits the view underlined by Catalano et al. (Catalano et al., 1998) suggesting that because in many brain systems class 3 semaphorins are not essential for their development, the *in vitro* response is not necessarily a good predictor of the *in vivo* phenotype resulting from knocking down the expression of semaphorins or their receptors. As a consequence of that complexity, more elaborate experiments involving multiple signaling pathways will be required to fully understand the role of Sema3F in the formation of the MTp.

Experimental Methods

Animals

Timed pregnant female Wistar rats (Charles Rivers) at embryonic day 14 (E14) were housed in single cages with ad-lib food and water. Nrp1 is critical for normal development (due in large measure to its role in VEGF signaling) and *Nrp1* null mice die at E10.5 – 12.5 (Gu et al., 2003; Kawasaki et al., 1999; Kitsukawa et al., 1997). To obtain mice lacking Nrp1 in TH expressing neurons (*Th-Cre*$^{+}$;*Nrp1*$^{c/c}$), floxed *Nrp1* mice obtained from Dr. David Ginty (Johns Hopkins University, Baltimore, MD) (Gu et al., 2003) were crossed with transgenic mice expressing Cre recombinase in all TH expressing cells (Gelman et al., 2003), thus excising the Nrp1 gene in those neurons only. These *TH-Nrp1* null mice are born in normal Mendelian ratio and are indistinguishable from their littermate controls. Nrp2 knockout mice were obtained from Dr. David Ginty (Johns Hopkins University, Baltimore, MD) and were generated by deleting exon 1 from the *Nrp2* gene (Giger et al., 2000). All protocols involving the use and maintenance of animals were approved by the Emory University Animal and Care Committee and conform to NIH guidelines.

Plasmids

The pBK-CMV expression vector containing Sema3A was generously provided by Dr. A. W. Puschel (Münster, Germany) (Adams et al., 1997; Puschel et al., 1995). A Sema3F expression vector was generously provided by Dr. M. Tessier-Lavigne (San Francisco) (Chen et al., 1997).

Stable Transfectants

293T cells were transfected with pBK-CMV-6×His/Flag-Sema3A, or pSecTag-alkaline phosphatase-Sema3F-myc/6×His, using Fugene® (Roche) according to the manufacturer's instructions. Stable cell lines were selected under G418 (250μl/ml) (Life Technology) or Zeocin (100 μg/ml) (Invitrogen). Expression of the fusion proteins was assessed by Western blot analysis and immunocytochemistry using monoclonal antibodies against myc (Roche), 6×His (Cell Signaling), Flag (Sigma) or human alkaline phosphatase.

Cell Cultures

Dissociated VM neuronal cultures were established from E14 rat embryos. The VM tissue extended about 1 mm at each side of the midline and for a millimeter rostral to the mesencephalic flexure. Tissue was incubated in Hank's buffered salt solution (H-BSS. Invitrogen) containing 0.25 % trypsin and 0.1mg/ml DNAse I (Sigma) for 15 minutes at 37° C, then triturated using polished glass pipettes, and plated on poly-L-lysine (PLL, Sigma) treated coverslips in MEM containing 10% Fetal Bovine Serum (FBS. Sigma). Coverslips were flipped over dishes containing 2-week-old VM astrocyte cultures, and incubated at 37°C in Neurobasal-A supplemented with B27 media (Invitrogen) for 2 to 14 days. Ten μM Cytosine-arabinoside (AraC. Sigma) were added 48 hrs after plating to control glia proliferation.

For growth cone collapse assays dissociated VM cells were allowed to aggregate using a modification of the hanging drop technique (Metin et al., 1997). Briefly, VM were dissected and trypsinized in the presence of 10 μM of the selective Rho-associated kinase (ROCK) inhibitor, Y-27632, since this compound appears to have a protective effect during the preparation and aggregation of human stem cells by reducing dissociation-induced apoptosis (Watanabe et al., 2007). VM dissociated cells were resuspended in MEM containing 0.2% Methocel (Recio-Pinto et al., 1986; Schlumpf et al., 1977), 10% horse serum and 10μM Y27632 and 20 μl aliquots containing 5×10^3 cells were allowed to aggregate for 1-2 days as hanging drops. Aggregates were plated on glass coverslips treated with 0.5 mg/ml PLL and 0.2μg/ml laminin. We found that this treatment leads to the rapid formation of large aggregates (24-48h) that readily adhered to the PLL/laminin-treated coverslips and promoted the formation of a profuse mantle rich in TH-positive axons. Culture was carried out in VM-glia conditioned Neurobasal A plus 1× B27 supplement containing 10μM AraC to prevent the proliferation of glial cells.

Co-cultures and repulsion assays

Control 293T cells and cells expressing Sema3A or Sema3F were grown in DMEM/10 % FBS media until confluence. Cells were trypsinized, dissociated and suspended in 5 ml of 10 % FBS/DMEM at 10^7 cells/ml. The cells were allowed to re-aggregate for 3 to 5 days. Aggregates were cut into approximately 500 μm diameter pieces for co-culture experiments. VM, brain stem (BrSt, tissue dissected caudal and lateral to the VM), and dorsal root ganglia (DRG) were obtained from E14 embryos. Hippocampal explants (Hc) were obtained from E16-E18 embryos, and used as positive controls for Sema3A/F co-cultures.

Pairs of tissue explants and stable 293T cell lines or untransfected 293T parent cell aggregates were placed 100-500 μm apart onto 24 well PLL treated dishes and embedded in a 1:1 mixture of collagen/Matrigel (Beckton and Dickinson). Collagen was mixed with 0.1 volume of 10 × MEM, 10% (v/v) fetal calf serum, before adding to Matrigel (Puschel et al., 1995). The collagen/Matrigel matrix (CM) was allowed to gel for 45 min at 37°C. Co-cultures were carried out for 2 days (DRG), or 5 days (VM, BrSt, or Hc) in Neurobasal A/B27 medium. DRG were cultured in the presence of 50 ng/ml 7S recombinant human nerve growth factor (Invitrogen). All cultures were treated with 10 μM AraC (Sigma) to inhibit the proliferation of astrocytes.

Affinity labeling of semaphorin receptors

Binding assays were carried out as described (Castellani et al., 2002) Untransfected 293 T cells (control) or stable 293T cell lines expressing Flag-tagged Sema3A or myc-tagged Sema3F were used. Cells were rinsed and incubated in fresh Neurobasal A/b27 medium. The secreted semaphorins were allowed to accumulate in the media for 3 to 5 days in culture. Conditioned media was pooled, filtered, and concentrated. Small aliquots were stored at -80°C until used. Sema3A, Sema3F, or control aliquots were diluted 10 fold for affinity labeling or growth cone collapse experiments. The formation of antigen/antibody complexes was promoted by the addition of a mouse anti-myc antibody to the Sema3F-conditioned media or either a rabbit anti-6×His or a goat anti Sema3A to the Sema3A-conditioned media, and incubated for 30 min at 37°C. Coverslips containing 2 and 5 days old VM neurons were overlaid with the complexes containing media and incubated for 30 minutes at 37°C. The neurons were rinsed several times with cold HBSS, fixed in 4% paraformaldehyde in 100 mM phosphate buffer (PB) and the complexes revealed with either an Alexa 488-conjugated goat anti mouse/rabbit or donkey anti goat secondary antibody. Cells were then permeabilized with 0.2% Triton X100 in PB and double-labeled with a rabbit anti-TH (Pell-Freez) to evaluate the co-localization of the complexes with vDA neurons.

Growth cone collapse assay

Collapse assays were performed on 5 day old VM cell aggregates prepared as described above. Conditioned media from semaphorin-expressing cells lines or untransfected 293T cells prepared as described above was diluted to 1× in Neurobasal A/B27 media. VM cell aggregates were incubated in this mix for 30 or 60 min followed by fixation in 4% paraformaldehyde in PB for 15 min. VM explants were double-stained for TH and α-tubulin to identify DA and non-DA axons. In some experiments, the actin cytoskeleton was labeled with Texas Red-conjugated Phalloidin. DA axons were identified by fluorescent microscopy and pictures were taken at 63× magnification. Growth cones growing free of any contact were selected (100 to 150 growth cones including lamellipodia and filopodia per explant) and their areas measured using ImageJ (NIH). In fully collapsed axons (a tapered axonal terminal without spread lamellipodia) the area was measured in the final 10 μm of the axonal tip.

Immunocytochemistry (ICC)

E14 embryos were fixed with 4% paraformaldehyde in PB, pH 7.4, cryoprotected in 30% sucrose in phosphate buffer, cut at 20 μm with a cryostat and mounted on gelatin coated glass slides. Cells and co-cultures were fixed in 4% paraformaldehyde, 4% sucrose in PB for 10 min, and permeabilized in 0.25% Triton X-100 for 5 minutes. Sections or cultured cells were processed for light or fluorescence immunocytochemistry with one of the following antibodies: goat anti-PlexinA1 (Santa Cruz at 1:10); goat anti-PlexinA3 V-15 (Santa Cruz at 1:50); rabbit anti PlexinA1 (Santa Cruz, 1:25); rabbit anti PlexinA3 (Santa Cruz, 1:25); rabbit anti Neuropilin1 1:500 (a generous gift from Dr. Fujisawa, Nagoya University, Nagoya, Japan); rabbit anti Neuropilin-2 (Santa Cruz, 1:50); rabbit anti PlexinA4, mouse anti NrCAM (Abcam, 1:500) and mouse anti L1CAM (Abcam, 1:500). Tissue sections and cultured neurons were double-stained by incubating them with one of the following antibodies: rabbit anti-TH (Pel-Freez, 1:500); mouse anti-TH (Sigma, 1:500), or mouse anti α-tubulin (Sigma, 1:10000). In some studies aimed to evaluate the organization of the vDA neurons and their projections we used a rabbit or sheep anti TH (Millipore) as described by Yamauchi et al. (Yamauchi et al., 2009). Incubation in the primary antibody combination was carried out overnight at 4°C. The localization of the different receptors was revealed by incubation with Alexa-conjugated and/or Cascade Blue conjugated secondary antibodies (Molecular Probes).

To assess the effect of Nrp1 or Nrp2 deletions on the development of the MTp pathways, TH-immunostained coronal, horizontal and parasagittal brain sections from knockout and control

strains were compared at E12, E14, E16, and adult. At early stages (E12), particular attention was paid to changes in the number and positioning of the DA neurons within the VM region as well as the organization of the DA fibers along the MTp. DA axons leaving the VM extend rostrally and fasciculate to form the MFB pathway before reaching the neostriatum. To identify MTp pathway defects, coronal, horizontal and parasagittal sections from each genotype (3-5 animals per genotype) were examined. To define defects in the antero-posterior, dorso-ventral and medio-lateral planes coronal sections were stained for TH as described above. The extension of aberrant DA axons growing caudally was also examined in parasagittal and coronal sections from embryonic and adult brain using the rabbit and goat anti TH antibodies (Millipore) as described by Yamauchi et al. (Yamauchi et al., 2009). Anatomical structures were identified by comparison to prenatal and adult mouse brain atlases (Schambra et al., 1991; Slotnik and Leonard, 1975)

Western Blotting

Western blots were carried out to verify the production of Sema3A, or Sema3F by stably transfected 293T cells. Conditioned media or cells were prepared in Laemmly buffer, loaded on 10% sodium dodecyl sulfate - polyacrylamide gels and transferred to nitrocellulose membranes (BioRad). Membranes were Ponceau-S stained to verify the uniformity of loads, blocked in 1× Odyssey blocking buffer, and then incubated with either mouse anti-Flag (Sigma), mouse anti-myc (Roche), or rabbit anti-6×His (Cell Signaling). The presence of the proteins was revealed using infrared-labeled secondary antibodies in a LI-COR Odyssey Infrared system.

Microscopy and Image documentation

Localization of semaphorins and semaphorin receptors was carried out in brain sections or VM dissociated cultures double-labeled with TH antibodies. Monochrome 8-bit digital images were acquired with a Retiga Exi (Q-Imaging) camera controlled by Simple PCI Imaging software. Acquisition parameters were adjusted such that the image could be taken in 0.1 seconds or faster. Staining intensity allowed the acquisition of images at gains smaller than 20 (range: 0.7-40). Images were further processed in Adobe Photoshop by adjusting saturation and contrast to best resemble the native immunostaining signal. Representative pictures from key areas are shown as single or merged images (Alexa 594, Alexa 488, Cascade blue/Hoechst). Confocal images were taken using a Zeiss LSM 510 confocal microscope equipped with META detectors and Argon and HENE/3PMT lasers.

MFB areas were measured in calibrated pictures comparable TH stained sagittal sections from E14 wild type and $Nrp2^{-/-}$ mouse brains using ImageJ. The areas were delimited between the top and bottom TH+ fiber crossing 500 μm wide segments traced from the end of the VM flexure to the Striatum. The width of the MFB was measured at the horizontal or vertical edge of each segment. Whole area was measured along the entire MFB starting at the rostral end of the VM flexure. Measurements from at least 3 sagittal sections were averaged for each animal (*wild type* n=3; $Nrp2^{-/-}$ n=2).

Behavioral tests

TH-Cre^{+};$Nrp1^{c/c}$, and $Nrp2^{-/-}$ knockout mice and their respective controls were subjected to two different behavioral tests: (A) Baseline locomotor activities were obtained at 3 month of age. Horizontal and vertical movements, rest time, total distances, and stereotypic activities were recorded using Versamax via Digiscan software (Accuscan Instruments, OH) over a period of 30 minutes. (B) Conditioned place preference (CPP): Place conditioning was performed using an unbiased CPP apparatus from Accuscan (Columbus, Ohio). On day 1, mice received a 30 minutes pre-test session during which they were allowed to freely explore the open field. Time spent in each compartment was recorded. The next 8 days, mice received 30

minute conditioning sessions during which the opening between the compartments is kept closed. On days 2, 4, 8 and 10 mice were placed in the non-preferred side chamber from the pre-test session following a s.c. injection of cocaine (5 mg/kg cocaine s.c.). On days 3, 5, 9 and 11 mice were placed in the preferred side chamber following a s.c. saline injection. On day 12, (test day) mice will be injected with saline, placed into the center of the box with access to all compartment. The amount of time spent in the compartment previously associated with the drug serves as an indicator of preference and a measure of reward learning. Five to 15 mice were used per test per genotype. CPP was calculated as the difference in the duration of time spent in the drug-paired compartment before and after drug conditioning. Mean beam crossing and CPP scores were compared using t-test.

Quantitative and Statistical analysis

The attractive or repulsive effect of semaphorins was measured as the ratio between the areas occupied by the proximal (P) and distal (D) half of the axonal halo emanating from tissue explants with respect to the 293T cell aggregate. Calibrated co-culture images taken at 2.5× or 10× were used to measure the P and D values using ImageJ (NIH) and to calculate a P/D value for each co-culture. The P/D value reflects the effect that a secreted molecule exerts over the direction and extent of axonal growth. Values larger than 100 indicate attraction while values smaller than 100 represent repulsion or inhibition. Only explants with unambiguous extension of neurites were measured. Since TH-staining provided an accurate view of the extent of the growth cone as judged by cultures double-stained with TH and Phalloidin, the collapse of the DA growth cone induced by semaphorins was measured by the reduction of the TH-stained growth cone area. Areas were measured in ImageJ (NIH) using calibrated images of TH stained cultures taken at 63× magnification. Statistical analyses were carried out in Kaleidagraph (Synergy Software). The areas were measured in several explants from at least three different cultures and compared using ANOVA followed by Student-Newman-Keuls post hoc test. P values < 0.05 were considered significantly different from control. Behavioral studies were compared by unpaired t test.

Acknowledgments

This work was supported by K08 NS46322-01A to R.E.G. E.R.T was partially supported by a Emory University URC and R03 NS048997 grants. We thank Elizabeth Jackson for her technical assistance and Su Li who conducted the CPP studies.

References

Troublesome variability in mouse studies. Nat Neurosci 2009;12:1075. [PubMed: 19710643]

Adams RH, Lohrum M, Klostermann A, Betz H, Puschel AW. The chemorepulsive activity of secreted semaphorins is regulated by furin-dependent proteolytic processing. Embo J 1997;16:6077–6086. [PubMed: 9321387]

Altman J, Bayer SA. Development of the brain stem in the rat. V. Thymidine-radiographic study of the time of origin of neurons in the midbrain tegmentum. The Journal of comparative neurology 1981;198:677–716. [PubMed: 7251936]

Bachelder RE, Lipscomb EA, Lin X, Wendt MA, Chadborn NH, Eickholt BJ, Mercurio AM. Competing autocrine pathways involving alternative neuropilin-1 ligands regulate chemotaxis of carcinoma cells. Cancer Res 2003;63:5230–5233. [PubMed: 14500350]

Bagri A, Marin O, Plump AS, Mak J, Pleasure SJ, Rubenstein JLR, Tessier-Lavigne M. Slit Proteins Prevent Midline Crossing and Determine the Dorsoventral Position of Major Axonal Pathways in the Mammalian Forebrain. Neuron 2002;33:233–248. [PubMed: 11804571]

Bagri A, Tessier-Lavigne M. Neuropilins as Semaphorin receptors: in vivo functions in neuronal cell migration and axon guidance. Adv Exp Med Biol 2002;515:13–31. [PubMed: 12613540]

Bals-Kubik R, Ableitner A, Herz A, Shippenberg TS. Neuroanatomical sites mediating the motivational effects of opioids as mapped by the conditioned place preference paradigm in rats. J Pharmacol Exp Ther 1993;264:489–495. [PubMed: 8093731]

Barnes G, Puranam RS, Luo Y, McNamara JO. Temporal specific patterns of semaphorin gene expression in rat brain after kainic acid-induced status epilepticus. Hippocampus 2003;13:1–20. [PubMed: 12625453]

Barzilai A, Zilkha-Falb R, Daily D, Stern N, Offen D, Ziv I, Melamed E, Shirvan A. The molecular mechanism of dopamine-induced apoptosis: identification and characterization of genes that mediate dopamine toxicity. J Neural Transm Suppl 2000:59–76. [PubMed: 11205158]

Bayer SA, Triarhou LC, Thomas JD, Ghetti B. Correlated quantitative studies of the neostriatum, nucleus accumbens, substantia nigra, and ventral tegmental area in normal and weaver mutant mice. J Neurosci 1994;14:6901–6910. [PubMed: 7965086]

Bayer SA, Wills KV, Triarhou LC, Ghetti B. Time of neuron origin and gradients of neurogenesis in midbrain dopaminergic neurons in the mouse. Exp Brain Res 1995;105:191–199. [PubMed: 7498372]

Belanger M, Auclair F, Bertrand L, Marchand R. The early neuronal organization predicts the path followed by some major axonal bundles in the embryonic brainstem. Neuroscience 1997;78:259–270. [PubMed: 9135106]

Benson DL, Colman DR, Huntley GW. Molecules, Maps And Synapse Specificity. Nat Rev Neurosci 2001;2

Betarbet R, Sherer TB, Greenamyre JT. Ubiquitin-proteasome system and Parkinson's diseases. Exp Neurol 2005;191:S17–S27. [PubMed: 15629758]

Brose K, Bland KS, Wang KH, Arnott D, Henzel W, Goodman CS, Tessier-Lavigne M, Kidd T. Slit proteins bind Robo receptors and have an evolutionarily conserved role in repulsive axon guidance. Cell 1999;96:795–806. [PubMed: 10102268]

Castellani V. The function of neuropilin/L1 complex. Adv Exp Med Biol 2002;515:91–102. [PubMed: 12613546]

Castellani V, Chedotal A, Schachner M, Faivre-Sarrailh C, Rougon G. Analysis of the L1-deficient mouse phenotype reveals cross-talk between Sema3A and L1 signaling pathways in axonal guidance. Neuron 2000;27:237–249. [PubMed: 10985345]

Castellani V, De Angelis E, Kenwrick S, Rougon G. Cis and trans interactions of L1 with neuropilin-1 control axonal responses to semaphorin 3A. Embo J 2002;21:6348–6357. [PubMed: 12456642]

Catalano A, Caprari P, Rodilossi S, Betta P, Castellucci M, Casazza A, Tamagnone L, Procopio A. Cross-talk between vascular endothelial growth factor and semaphorin-3A pathway in the regulation of normal and malignant mesothelial cell proliferation. Faseb J 2004;18:358–360. [PubMed: 14656993]

Catalano SM, Messersmith EK, Goodman CS, Shatz CJ, Chedotal A. Many major CNS axon projections develop normally in the absence of semaphorin III. Mol Cell Neurosci 1998;11:173–182. [PubMed: 9675049]

Chen G, Sima J, Jin M, Wang KY, Xue XJ, Zheng W, Ding YQ, Yuan XB. Semaphorin-3A guides radial migration of cortical neurons during development. Nat Neurosci 2008;11:36–44. [PubMed: 18059265]

Chen H, Bagri A, Zupicich JA, Zou Y, Stoeckli E, Pleasure SJ, Lowenstein DH, Skarnes WC, Chedotal A, Tessier-Lavigne M. Neuropilin-2 regulates the development of selective cranial and sensory nerves and hippocampal mossy fiber projections. Neuron 2000;25:43–56. [PubMed: 10707971]

Chen H, Chedotal A, He Z, Goodman CS, Tessier-Lavigne M. Neuropilin-2, a novel member of the neuropilin family, is a high affinity receptor for the semaphorins Sema E and Sema IV but not Sema III. Neuron 1997;19:547–559. [PubMed: 9331348]

Chen H, He Z, Bagri A, Tessier-Lavigne M. Semaphorin-neuropilin interactions underlying sympathetic axon responses to class III semaphorins. Neuron 1998a;21:1283–1290. [PubMed: 9883722]

Chen H, He Z, Tessier-Lavigne M. Axon guidance mechanisms: semaphorins as simultaneous repellents and anti-repellents. Nat Neurosci 1998b;1:436–439. [PubMed: 10196539]

Cheng HJ, Bagri A, Yaron A, Stein E, Pleasure SJ, Tessier-Lavigne M. Plexin-A3 mediates semaphorin signaling and regulates the development of hippocampal axonal projections. Neuron 2001;32:249–263. [PubMed: 11683995]

Cloutier JF, Giger RJ, Koentges G, Dulac C, Kolodkin AL, Ginty DD. Neuropilin-2 mediates axonal fasciculation, zonal segregation, but not axonal convergence, of primary accessory olfactory neurons. Neuron 2002;33:877–892. [PubMed: 11906695]

Dahlstrand J, Lardelli M, Lendahl U. Nestin mRNA expression correlates with the central nervous system progenitor cell state in many, but not all, regions of developing central nervous system. Brain Res Dev Brain Res 1995;84:109–129.

Demyanenko G, Shibata Y, Maness P. Altered distribution of dopaminergic neurons in the brain of L1 null mice. Brain Res Dev Brain Res 2001;126:21.

Deo RC, Schmidt EF, Elhabazi A, Togashi H, Burley SK, Strittmatter SM. Structural bases for CRMP function in plexin-dependent semaphorin3A signaling. Embo J 2004;23:9–22. [PubMed: 14685275]

Di Monte DA. The environment and Parkinson's disease: is the nigrostriatal system preferentially targeted by neurotoxins? Lancet Neurol 2003;2:531–538. [PubMed: 12941575]

Dontchev VD, Letourneau PC. Nerve growth factor and semaphorin 3A signaling pathways interact in regulating sensory neuronal growth cone motility. J Neurosci 2002;22:6659–6669. [PubMed: 12151545]

Eickholt BJ, Mackenzie SL, Graham A, Walsh FS, Doherty P. Evidence for collapsin-1 functioning in the control of neural crest migration in both trunk and hindbrain regions. Development (Cambridge, England) 1999;126:2181–2189.

Falk J, Bechara A, Fiore R, Nawabi H, Zhou H, Hoyo-Becerra C, Bozon M, Rougon G, Grumet M, Puschel AW, Sanes JR, Castellani V. Dual functional activity of semaphorin 3B is required for positioning the anterior commissure. Neuron 2005;48:63–75. [PubMed: 16202709]

Flores C, Manitt C, Rodaros D, Thompson KM, Rajabi H, Luk KC, Tritsch NX, Sadikot AF, Stewart J, Kennedy TE. Netrin receptor deficient mice exhibit functional reorganization of dopaminergic systems and do not sensitize to amphetamine. Mol Psychiatry 2005;10:606–612. [PubMed: 15534618]

Fu SY, Sharma K, Luo Y, Raper JA, Frank E. SEMA3A regulates developing sensory projections in the chicken spinal cord. J Neurobiol 2000;45:227–236. [PubMed: 11077427]

Funato H, Saito-Nakazato Y, Takahashi H. Axonal growth from the habenular nucleus along the neuromere boundary region of the diencephalon is regulated by semaphorin 3F and netrin-1. Mol Cell Neurosci 2000;16:206–220. [PubMed: 10995548]

Garcez PP, Henrique NP, Furtado DA, Bolz J, Lent R, Uziel D. Axons of callosal neurons bifurcate transiently at the white matter before consolidating an interhemispheric projection. Eur J Neurosci 2007;25:1384–1394. [PubMed: 17425565]

Gates MA, Coupe VM, Torres EM, Fricker-Gates RA, Dunnet SB. Spatially and tewmporally restricted chemoattractive and chemorepulsice cues direct the formation of the nigro-straiatal system circuit. Eur J Neurosci 2004;19:831–844. [PubMed: 15009130]

Gelman DM, Noain D, Avale ME, Otero V, Low MJ, Rubinstein M. Transgenic mice engineered to target Cre/loxP-mediated DNA recombination into catecholaminergic neurons. Genesis 2003;36:196–202. [PubMed: 12929090]

Gerlai R. Gene-targeting studies of mammalian behavior: is it the mutation or the background genotype? Trends Neurosci 1996;19:177–181. [PubMed: 8723200]

Giger RJ, Cloutier JF, Sahay A, Prinjha RK, Levengood DV, Moore SE, Pickering S, Simmons D, Rastan S, Walsh FS, Kolodkin AL, Ginty DD, Geppert M. Neuropilin-2 is required in vivo for selective axon guidance responses to secreted semaphorins. Neuron 2000;25:29–41. [PubMed: 10707970]

Gong S, Doughty M, Harbaugh CR, Cummins A, Hatten ME, Heintz N, Gerfen CR. Targeting Cre recombinase to specific neuron populations with bacterial artificial chromosome constructs. J Neurosci 2007;27:9817–9823. [PubMed: 17855595]

Goshima Y, Ito T, Sasaki Y, Nakamura F. Semaphorins as signals for cell repulsion and invasion. J Clin Invest 2002;109:993–998. [PubMed: 11956234]

Goshima Y, Sasaki Y, Nakayama T, Ito T, Kimura T. Functions of semaphorins in axon guidance and neuronal regeneration. Jpn J Pharmacol 2000;82:273–279. [PubMed: 10875745]

Gruber C, Kahl A, Lebenheim L, Kowski A, Dittgen A, Veh RW. Dopaminergic projections from the VTA substantially contribute to the mesohabenular pathway in the rat. Neurosci Lett 2007;427:165–170. [PubMed: 17949902]

Gu C, Rodriguez ER, Reimert DV, Shu T, Fritzsch B, Richards LJ, Kolodkin AL, Ginty DD. Neuropilin-1 conveys semaphorin and VEGF signaling during neural and cardiovascular development. Dev Cell 2003;5:45–57. [PubMed: 12852851]

Haber SN. The primate basal ganglia: parallel and integrative networks. J Chem Neuroanat 2003;26:317–330. [PubMed: 14729134]

Hague SM, Klaffke S, Bandmann O. Neurodegenerative disorders: Parkinson's disease and Huntington's disease. J Neurol Neurosurg Psychiatry 2005;76:1058–1063. [PubMed: 16024878]

Henion TR, Schwarting GA. Patterning the developing and regenerating olfactory system. J Cell Physiol 2007;210:290–297. [PubMed: 17111357]

Hernandez-Montiel HL, Tamariz E, Sandoval-Minero MT, Varela-Echavarria A. Semaphorins 3A, 3C, and 3F in mesencephalic dopaminergic axon pathfinding. J Comp Neurol 2008;506:387–397. [PubMed: 18041777]

Horinouchi K, Nakamura Y, Yamanaka H, Watabe T, Shiosaka S. Distribution of L1cam mRNA in the adult mouse brain: In situ hybridization and Northern blot analyses. The Journal of comparative neurology 2005;482:386–404. [PubMed: 15669056]

Huber AB, Kolodkin AL, Ginty DD, Cloutier JF. SIGNALING AT THE GROWTH CONE: Ligand-Receptor Complexes and the Control of Axon Growth and Guidance. Ann Rev Neurosci 2003;26:509–563. [PubMed: 12677003]

Hulley P, Schachner M, Lubbert H. L1 neural cell adhesion molecule is a survival factor for fetal dopaminergic neurons. J Neurosci Res 1998;53:129–134. [PubMed: 9671969]

Imai T, Yamazaki T, Kobayakawa R, Kobayakawa K, Abe T, Suzuki M, Sakano H. Pre-target axon sorting establishes the neural map topography. Science 2009;325:585–590. [PubMed: 19589963]

Joel D, Weiner I. The connections of the dopaminergic system with the striatum in rats and primates: an analysis with respect to the functional and compartmental organization of the striatum. Neuroscience 2000;96:451–474. [PubMed: 10717427]

Kawano H, Horie M, Honma S, Kawamura K, Takeuchi K, Kimura S. Aberrant trajectory of ascending dopaminergic pathway in mice lacking Nkx2.1. Exp Neurol 2003;182:103–112. [PubMed: 12821380]

Kawano H, Ohyama K, Kawamura K, Nagatsu I. Migration of dopaminergic neurons in the embryonic mesencephalon of mice. Brain Res Dev Brain Res 1995;86:101–113.

Kawasaki T, Bekku Y, Suto F, Kitsukawa T, Taniguchi M, Nagatsu I, Nagatsu T, Itoh K, Yagi T, Fujisawa H. Requirement of neuropilin 1-mediated Sema3A signals in patterning of the sympathetic nervous system. Development (Cambridge, England) 2002;129:671–680.

Kawasaki T, Kitsukawa T, Bekku Y, Matsuda Y, Sanbo M, Yagi T, Fujisawa H. A requirement for neuropilin-1 in embryonic vessel formation. Development (Cambridge, England) 1999;126:4895–4902.

Kitsukawa T, Shimizu M, Sanbo M, Hirata T, Taniguchi M, Bekku Y, Yagi T, Fujisawa H. Neuropilin-semaphorin III/D-mediated chemorepulsive signals play a crucial role in peripheral nerve projection in mice. Neuron 1997;19:995–1005. [PubMed: 9390514]

Knoll B, Drescher U. Ephrin-As as receptors in topographic projections. Trends Neurosci 2002;25:145–149. [PubMed: 11852146]

Kolk SM, Gunput RA, Tran TS, van den Heuvel DM, Prasad AA, Hellemons AJ, Adolfs Y, Ginty DD, Kolodkin AL, Burbach JP, Smidt MP, Pasterkamp RJ. Semaphorin 3F is a bifunctional guidance cue for dopaminergic axons and controls their fasciculation, channeling, rostral growth, and intracortical targeting. J Neurosci 2009;29:12542–12557. [PubMed: 19812329]

Kurschat P, Bielenberg D, Rossignol-Tallandier M, Stahl A, Klagsbrun M. Neuron restrictive silencer factor NRSF/REST is a transcriptional repressor of neuropilin-1 and diminishes the ability of semaphorin 3A to inhibit keratinocyte migration. J Biol Chem 2006;281(5):2721–2729. [PubMed: 16330548]

Lein ES, Hawrylycz MJ, Ao N, Ayres M, Bensinger A, Bernard A, Boe AF, Boguski MS, Brockway KS, Byrnes EJ, Chen L, Chen TM, Chin MC, Chong J, Crook BE, Czaplinska A, Dang CN, Datta S, Dee NR, Desaki AL, Desta T, Diep E, Dolbeare TA, Donelan MJ, Dong HW, Dougherty JG, Duncan BJ, Ebbert AJ, Eichele G, Estin LK, Faber C, Facer BA, Fields R, Fischer SR, Fliss TP, Frensley C, Gates SN, Glattfelder KJ, Halverson KR, Hart MR, Hohmann JG, Howell MP, Jeung DP, Johnson RA,

Karr PT, Kawal R, Kidney JM, Knapik RH, Kuan CL, Lake JH, Laramee AR, Larsen KD, Lau C, Lemon TA, Liang AJ, Liu Y, Luong LT, Michaels J, Morgan JJ, Morgan RJ, Mortrud MT, Mosqueda NF, Ng LL, Ng R, Orta GJ, Overly CC, Pak TH, Parry SE, Pathak SD, Pearson OC, Puchalski RB, Riley ZL, Rockett HR, Rowland SA, Royall JJ, Ruiz MJ, Sarno NR, Schaffnit K, Shapovalova NV, Sivisay T, Slaughterbeck CR, Smith SC, Smith KA, Smith BI, Sodt AJ, Stewart NN, Stumpf KR, Sunkin SM, Sutram M, Tam A, Teemer CD, Thaller C, Thompson CL, Varnam LR, Visel A, Whitlock RM, Wohnoutka PE, Wolkey CK, Wong VY, Wood M, Yaylaoglu MB, Young RC, Youngstrom BL, Yuan XF, Zhang B, Zwingman TA, Jones AR. Genome-wide atlas of gene expression in the adult mouse brain. Nature 2007;445:168–176. [PubMed: 17151600]

Leonardo ED, Hinck L, Masu M, Keino-Masu K, Fazeli A, Stoeckli ET, Ackerman SL, Weinberg RA, Tessier-Lavigne M. Guidance of developing axons by netrin-1 and its receptors. Cold Spring Harb Symp Quant Biol 1997;62:467–478. [PubMed: 9598381]

Lim KL, Lim TM. Molecular mechanisms of neurodegeneration in Parkinson's disease: clues from Mendelian syndromes. IUBMB Life 2003;55:315–322. [PubMed: 12938733]

Lin L, Isacson O. Axonal growth regulation of fetal and embryonic stem cell-derived dopaminergic neurons by Netrin-1 and Slits. Stem Cells 2006;24:2504–2513. [PubMed: 16840550]

Lin L, Rao Y, Isacson O. Netrin-1 and slit-2 regulate and direct neurite growth of ventral midbrain dopaminergic neurons. Mol Cell Neurosci 2005;28:547–555. [PubMed: 15737744]

Lindwall C, Fothergill T, Richards LJ. Commissure formation in the mammalian forebrain. Curr Opin Neurobiol 2007;17:3–14. [PubMed: 17275286]

MacLennan AJ, McLaurin DL, Marks L, Vinson EN, Pfeifer M, Szulc SV, Heaton MB, Lee N. Immunohistochemical localization of netrin-1 in the embryonic chick nervous system. J Neurosci 1997;17:5466–5479. [PubMed: 9204929]

Marillat V, Cases O, Nguyen-Ba-Charvet KT, Tessier-Lavigne M, Sotelo C, Chedotal A. Spatiotemporal expression patterns of slit and robo genes in the rat brain. The Journal of comparative neurology 2002;442:130–155. [PubMed: 11754167]

Mastick GS, Easter SS Jr. Initial Organization of Neurons and Tracts in the Embryonic Mouse Fore- and Midbrain. Dev Biol 1996;173:79–94. [PubMed: 8575640]

Masuda T, Tsuji H, Taniguchi M, Yagi T, Tessier-Lavigne M, Fujisawa H, Okado N, Shiga T. Differential non-target-derived repulsive signals play a critical role in shaping initial axonal growth of dorsal root ganglion neurons. Dev Biol 2003;254:289–302. [PubMed: 12591248]

Melendez-Herrera E, Varela-Echavarria A. Expression of secreted semaphorins and their receptors in specific neuromeres, boundaries, and neuronal groups in the developing mouse and chick brain. Brain Res 2006;1067:126–137. [PubMed: 16360650]

Metin C, Deleglise D, Serafini T, Kennedy TE, Tessier-Lavigne M. A role for netrin-1 in the guidance of cortical efferents. Development 1997;124:5063–5074. [PubMed: 9362464]

Mitsui N, Inatome R, Takahashi S, Goshima Y, Yamamura H, Yanagi S. Involvement of Fes/Fps tyrosine kinase in semaphorin3A signaling. Embo J 2002;21:3274–3285. [PubMed: 12093729]

Moore DJ, West AB, Dawson VL, Dawson TM. Molecular pathophysiology of Parkinson's disease. Annu Rev Neurosci 2005;28:57–87. [PubMed: 16022590]

Munakata H, Nakamura Y, Matsumoto-Miyai K, Itoh K, Yamasaki H, Shiosaka S. Distribution and densitometry mapping of L1-CAM immunoreactivity in the adult mouse brain--light microscopic observation. BMC Neurosci 2003;4:7. [PubMed: 12697052]

Nakamura F, Kalb RG, Strittmatter SM. Molecular basis of semaphorin-mediated axon guidance. J Neurobiol 2000a;44:219–229. [PubMed: 10934324]

Nakamura S, Ito Y, Shirasaki R, Murakami F. Local Directional Cues Control Growth Polarity of Dopaminergic Axons Along the Rostrocaudal Axis. J Neurosci 2000b;20:4112–4119. [PubMed: 10818146]

Nasarre P, Constantin B, Rouhaud L, Harnois T, Raymond G, Drabkin HA, Bourmeyster N, Roche J. Semaphorin SEMA3F and VEGF have opposing effects on cell attachment and spreading. Neoplasia 2003;5:83–92. [PubMed: 12659673]

Niclou SP, Jia L, Raper JA. Slit2 is a repellent for retinal ganglion cell axons. J Neurosci 2000;20:4962–4974. [PubMed: 10864954]

Ohyama K, Kawano H, Asou H, Fukuda T, Oohira A, Uyemura K, K K. Coordinate expression of L1 and 6B4 proteoglycan/phosphacan is correlated with the migration of mesencephalic dopaminergic neurons in mice. Brain Res Dev Brain Res 1998;107:219.

Osborne NJ, Begbie J, Chilton JK, Schmidt H, Eickholt BJ. Semaphorin/neuropilin signaling influences the positioning of migratory neural crest cells within the hindbrain region of the chick. Dev Dyn 2005a;232:939–949. [PubMed: 15729704]

Osborne PB, Halliday GM, Cooper HM, Keast JR. Localization of immunoreactivity for deleted in colorectal cancer (DCC), the receptor for the guidance factor netrin-1, in ventral tier dopamine projection pathways in adult rodents. Neuroscience 2005b;131:671–681. [PubMed: 15730872]

Park D, Xiang AP, Zhang L, Mao FF, Walton NM, Choi SS, Lahn BT. The radial glia antibody RC2 recognizes a protein encoded by Nestin. Biochem Biophys Res Commun 2009;382:588–592. [PubMed: 19302980]

Perrone-Capano C, Di Porzio U. Genetic and epigenetic control of midbrain dopaminergic neuron development. Int J Dev Biol 2000;44:679–687. [PubMed: 11061432]

Phillips TJ, Hen R, Crabbe JC. Complications associated with genetic background effects in research using knockout mice. Psychopharmacology (Berl) 1999;147:5–7. [PubMed: 10591855]

Phillipson O, Griffith A. The neurones of origin for the mesohabenular dopamine pathway. Brain Res 1980;197:213–218. [PubMed: 7397554]

Potiron VA, Sharma G, Nasarre P, Clarhaut JA, Augustin HG, Gemmill RM, Roche J, Drabkin HA. Semaphorin SEMA3F affects multiple signaling pathways in lung cancer cells. Cancer Res 2007;67:8708–8715. [PubMed: 17875711]

Price DJ, Kennedy H, Dehay C, Zhou L, Mercier M, Jossin Y, Goffinet AM, Tissir F, Blakey D, Molnar Z. The development of cortical connections. Eur J Neurosci 2006;23:910–920. [PubMed: 16519656]

Puschel AW, Adams RH, Betz H. Murine semaphorin D/collapsin is a member of a diverse gene family and creates domains inhibitory for axonal extension. Neuron 1995;14:941–948. [PubMed: 7748561]

Recio-Pinto E, Rechler MM, Ishii DN. Effects of insulin, insulin-like growth factor-II, and nerve growth factor on neurite formation and survival in cultured sympathetic and sensory neurons. J Neurosci 1986;6:1211–1219. [PubMed: 3519887]

Rohm B, Ottemeyer A, Lohrum M, Puschel AW. Plexin/neuropilin complexes mediate repulsion by the axonal guidance signal semaphorin 3A. Mech Dev 2000a;93:95–104. [PubMed: 10781943]

Rohm B, Rahim B, Kleiber B, Hovatta I, Puschel AW. The semaphorin 3A receptor may directly regulate the activity of small GTPases. FEBS Lett 2000b;486:68–72. [PubMed: 11108845]

Sahay A, Molliver ME, Ginty DD, Kolodkin AL. Semaphorin 3F is critical for development of limbic system circuitry and is required in neurons for selective CNS axon guidance events. J Neurosci 2003;23:6671–6680. [PubMed: 12890759]

Scarlato M, Ara J, Bannerman P, Scherer S, Pleasure D. Induction of neuropilins-1 and -2 and their ligands, Sema3A, Sema3F, and VEGF, during Wallerian degeneration in the peripheral nervous system. Exp Neurol 2003;183:489–498. [PubMed: 14552889]

Schambra UB, Silver J, Lauder JM. An atlas of the prenatal mouse brain: gestational day 14. Exp Neurol 1991;114:145–183. [PubMed: 1748192]

Schlumpf M, Shoemaker WJ, Bloom FE. Explant cultures of catecholamine-containing neurons from rat brain: biochemical, histofluorescence, and electron microscopic studies. Proc Natl Acad Sci U S A 1977;74:4471–4475. [PubMed: 270693]

Shimizu A, Mammoto A, Italiano JE Jr, Pravda E, Dudley AC, Ingber DE, Klagsbrun M. ABL2/ARG tyrosine kinase mediates SEMA3F-induced RhoA inactivation and cytoskeleton collapse in human glioma cells. J Biol Chem 2008;283:27230–27238. [PubMed: 18660502]

Shirasaki R, Mirzayan C, Tessier-Lavigne M, Murakami F. Guidance of circumferentially growing axons by netrin-dependent and -independent floor plate chemotropism in the vertebrate brain. Neuron 1996;17:1079–1088. [PubMed: 8982157]

Shults C, Hashimoto R, Brady R, Gage F. Dopaminergic cells align along radial glia in the developing mesencephalon of the rat. Neuroscience 1990;38:427–436. [PubMed: 1979855]

Skagerberg G, Lindvall O, Bjorklund A. Origin, course and termination of the mesohabenular dopamine pathway in the rat. Brain Res 1984;307:99–108. [PubMed: 6087992]

Slotnik, BM.; Leonard, CM. A stereotaxic atlas of the albino mouse forebrain. U.S. Dept. of Health, Education, and Welfare, Public Health Service, Alcohol, Drug Abuse, and Mental Health Administration; Rockville, Md, Washington: 1975.

Spassky N, de Castro F, Le Bras B, Heydon K, Queraud-LeSaux F, Bloch-Gallego E, Chedotal A, Zalc B, Thomas JL. Directional guidance of oligodendroglial migration by class 3 semaphorins and netrin-1. J Neurosci 2002;22:5992–6004. [PubMed: 12122061]

Steward O, Trimmer PA. Genetic influences on cellular reactions to CNS injury: the reactive response of astrocytes in denervated neuropil regions in mice carrying a mutation (Wld(S)) that causes delayed Wallerian degeneration. J Comp Neurol 1997;380:70–81. [PubMed: 9073083]

Suto F, Ito K, Uemura M, Shimizu M, Shinkawa Y, Sanbo M, Shinoda T, Tsuboi M, Takashima S, Yagi T, Fujisawa H. Plexin-a4 mediates axon-repulsive activities of both secreted and transmembrane semaphorins and plays roles in nerve fiber guidance. J Neurosci 2005;25:3628–3637. [PubMed: 15814794]

Suto F, Murakami Y, Nakamura F, Goshima Y, Fujisawa H. Identification and characterization of a novel mouse plexin, plexin-A4. Mech Dev 2003;120:385–396. [PubMed: 12591607]

Suto F, Tsuboi M, Kamiya H, Mizuno H, Kiyama Y, Komai S, Shimizu M, Sanbo M, Yagi T, Hiromi Y, Chedotal A, Mitchell KJ, Manabe T, Fujisawa H. Interactions between plexin-A2, plexin-A4, and semaphorin 6A control lamina-restricted projection of hippocampal mossy fibers. Neuron 2007;53:535–547. [PubMed: 17296555]

Takahashi T, Fournier A, Nakamura F, Wang LH, Murakami Y, Kalb RG, Fujisawa H, Strittmatter SM. Plexin-neuropilin-1 complexes form functional semaphorin-3A receptors. Cell 1999;99:59–69. [PubMed: 10520994]

Takahashi T, Strittmatter SM. Plexina1 autoinhibition by the plexin sema domain. Neuron 2001;29:429–439. [PubMed: 11239433]

Tamamaki N, Fujimori K, Nojyo Y, Kaneko T, Takauji R. Evidence that Sema3A and Sema3F regulate the migration of GABAergic neurons in the developing neocortex. The Journal of comparative neurology 2003;455:238–248. [PubMed: 12454988]

Taniguchi M, Yuasa S, Fujisawa H, Naruse I, Saga S, Mishina M, Yagi T. Disruption of semaphorin III/D gene causes severe abnormality in peripheral nerve projection. Neuron 1997;19:519–530. [PubMed: 9331345]

Tessier-Lavigne M, Goodman CS. The molecular biology of axon guidance. Science 1996;274:1123–1133. [PubMed: 8895455]

Tsai HH, Miller RH. Glial cell migration directed by axon guidance cues. Trends Neurosci 2002;25:173–175. discussion 175-176. [PubMed: 11998681]

Tzschentke TM. Measuring reward with the conditioned place preference paradigm: a comprehensive review of drug effects, recent progress and new issues. Prog Neurobiol 1998;56:613–672. [PubMed: 9871940]

Vitalis T, Cases O, Engelkamp D, Verney C, Price DJ. Defect of tyrosine hydroxylase-immunoreactive neurons in the brains of mice lacking the transcription factor Pax6. J Neurosci 2000;20:6501–6516. [PubMed: 10964956]

Voorn P, Kalsbeek A, Jorritsma-Byham B, Groenewegen HJ. The pre- and postnatal deveelopment of the dopaminergic cell groups in the ventral mesencephalon and the dopaminergic innervation of the striatum. Neuroscience 1988;25:857–887. [PubMed: 3405431]

Watanabe K, Ueno M, Kamiya D, Nishiyama A, Matsumura M, Wataya T, Takahashi JB, Nishikawa S, Nishikawa S, Muguruma K, Sasai Y. A ROCK inhibitor permits survival of dissociated human embryonic stem cells. Nat Biotechnol 2007;25:681–686. [PubMed: 17529971]

Webber A, Raz Y. Axon guidance cues in auditory development. Anat Rec A Discov Mol Cell Evol Biol 2006;288:390–396. [PubMed: 16550548]

Wei LC, Shi M, Chen LW, Cao R, Zhang P, Chan YS. Nestin-containing cells express glial fibrillary acidic protein in the proliferative regions of central nervous system of postnatal developing and adult mice. Brain Res Dev Brain Res 2002;139:9–17.

Winberg ML, Mitchell KJ, Goodman CS. Genetic analysis of the mechanisms controlling target selection: complementary and combinatorial functions of netrins, semaphorins, and IgCAMs. Cell 1998;93:581–591. [PubMed: 9604933]

Wright AG, Demyanenko GP, Powell A, Schachner M, Enriquez-Barreto L, Tran TS, Polleux F, Maness PF. Close homolog of L1 and neuropilin 1 mediate guidance of thalamocortical axons at the ventral telencephalon. J Neurosci 2007;27:13667–13679. [PubMed: 18077678]

Yamauchi K, Mizushima S, Tamada A, Yamamoto N, Takashima S, Murakami F. FGF8 signaling regulates growth of midbrain dopaminergic axons by inducing semaphorin 3F. J Neurosci 2009;29:4044–4055. [PubMed: 19339600]

Yaron A, Huang PH, Cheng HJ, Tessier-Lavigne M. Differential requirement for Plexin-A3 and -A4 in mediating responses of sensory and sympathetic neurons to distinct class 3 Semaphorins. Neuron 2005;45:513–523. [PubMed: 15721238]

Yue Y, Widmer DA, Halladay AK, Cerretti DP, Wagner GC, Dreyer JL, Zhou R. Specification of distinct dopaminergic neural pathways: roles of the Eph family receptor EphB1 and ligand ephrin-B2. J Neurosci 1999;19:2090–2101. [PubMed: 10066262]

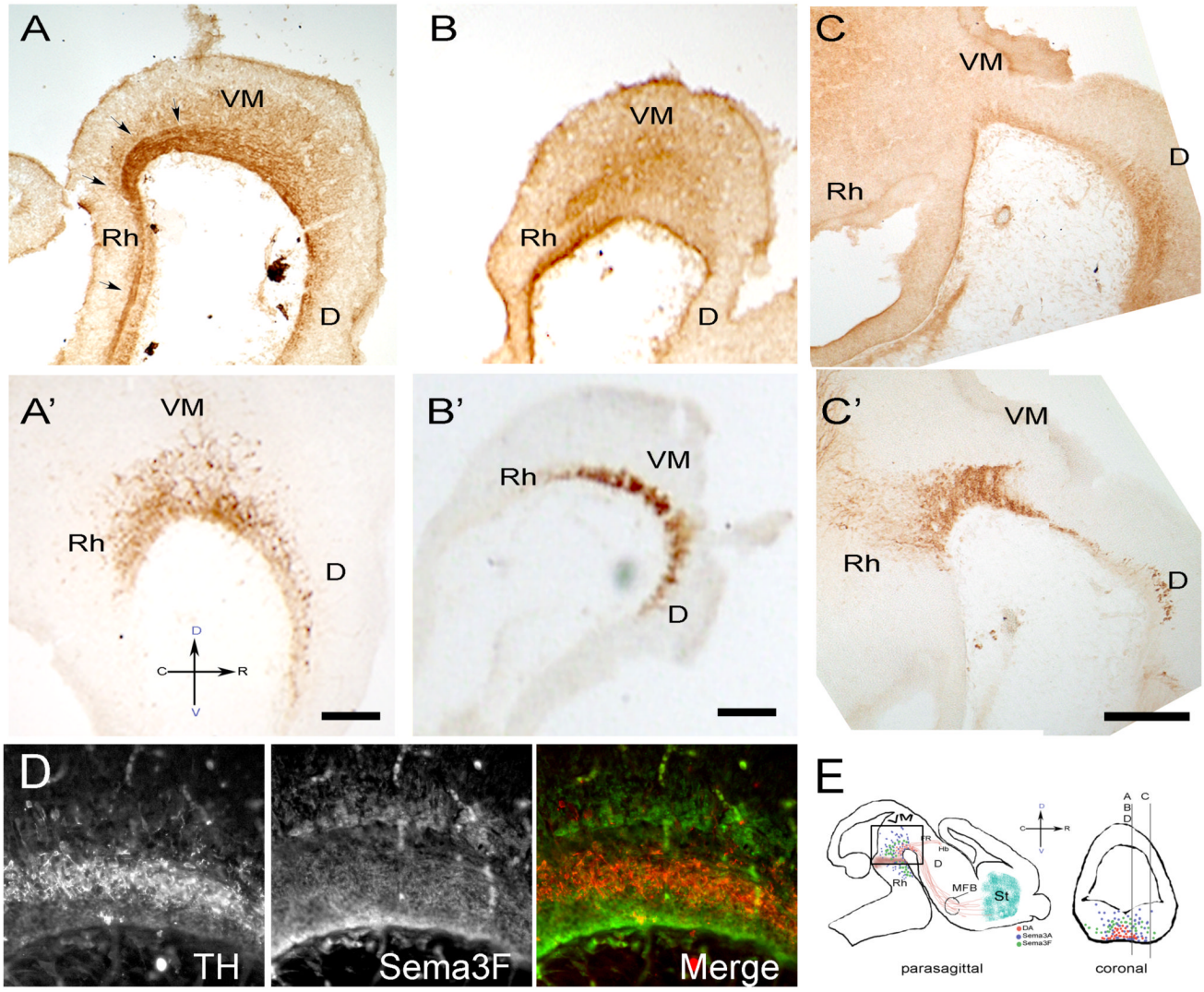

Figure 1. Sema3A and Sema3F are strongly expressed in the ventral mesencephalon of E13.5 VM rat embryos

E13.5 rat embryos were fixed and 40μm adjacent sagittal sections were stained with antibodies against Sema3A (A), Sema3F (B, C) or TH (A′, B′, C′). In the VM (A), Sema3A is found as an increasing gradient extending from the floor of the ventricle to the pial surface. Medial sections showed a dense track of axons originating in the rostral mesencephalon, presumably the medial longitudinal fasciculus, which was strongly stained for Sema3A (arrows). Sema3F is expressed in a region that appears to wrap the DA neurons at their dorsal, ventral and caudal borders while presenting an ostensibly decreasing gradient in the rostral direction. The caging pattern dissipates in lateral regions of the VM (C). (D) Double staining with TH (red) and Sema3F (green) antibodies confirms the caging distribution of Sema3F. (E) Schematic diagram of the sectioning strategy used along these studies. Stained sections were cut parasagittally within 500 μm from the midline as represented in a coronal section for panels A, B, C and D. All pictures were taken in the region depicted by the frame in the sagittal cut. Spatial orientation is represented by a cross where C, R, D, and V represent caudal, rostral, dorsal and ventral positions. Scale bars: 100 μm. D, Diencephalon; Rh, Rhomboencephalon; FR, fasciculus retroflexus; Hb, habenula.

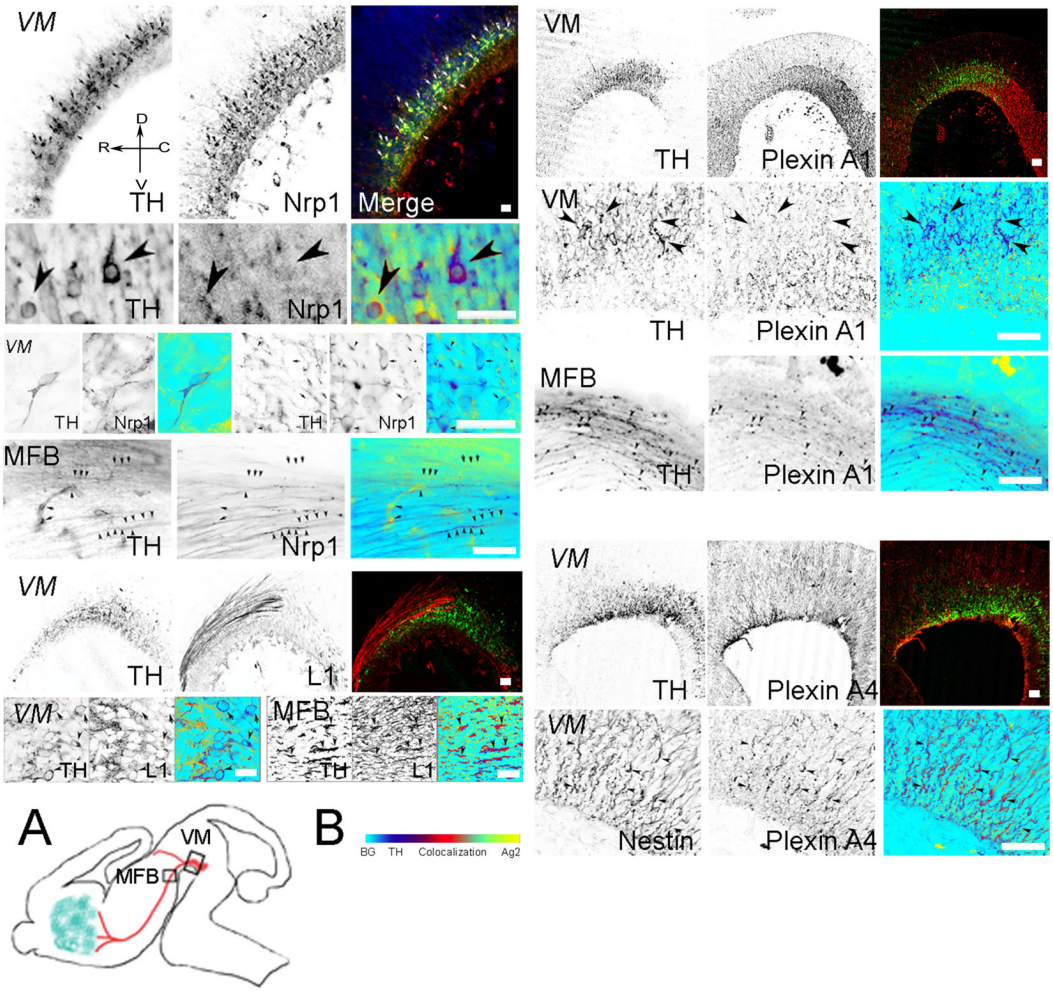

Figure 2. Expression of Sema3A receptor components *in vivo*

The Sema3A receptor complex comprises Neuropilin 1 (Nrp1), PlexinA1 and/or A4, and L1CAM (L1). The figure shows the immunolocalization of the individual components of the Sema3A receptor in the VM of E13.5 rat. Embryos were fixed and 20μm sagittal sections were cut within the region depicted in fig. 1 and double-stained with antibodies against TH (green) and Nrp1, L1, PlexinA1 or PlexinA4 (red). Green and red signal co-localization is shown in the merge panel. For some pictures the merging process was made in Photoshop by placing an inverted copy of the red channel image in the blue channel while the green channel image was inverted, rendering a merged picture where TH is shown in blue, the second antigen in yellow while co-localization varies from light green to red (arrowheads). Nrp1, as well as PlexinA1 immunorectivity was generally in a light punctate pattern that co-localized with a low number of TH-stained cells in the VM and fibers in the medial forebrain bundle (MFB). L1 immunoreactivity strongly stained non-TH fibers extending out of the VM and was frequently associated with DA neurons and their fibers in the MFB. In contrast, PlexinA4 did not stain vDA neurons or their axons but it co-localized with radial glia in the VM as suggested by its co-localization with Nestin. (A) Diagram showing the regions where the VM or MFB pictures were taken. (B) Co-localization bar. Picture orientation is represented by the orientation cross in the top left panel. Calibration bars: 50 μm.

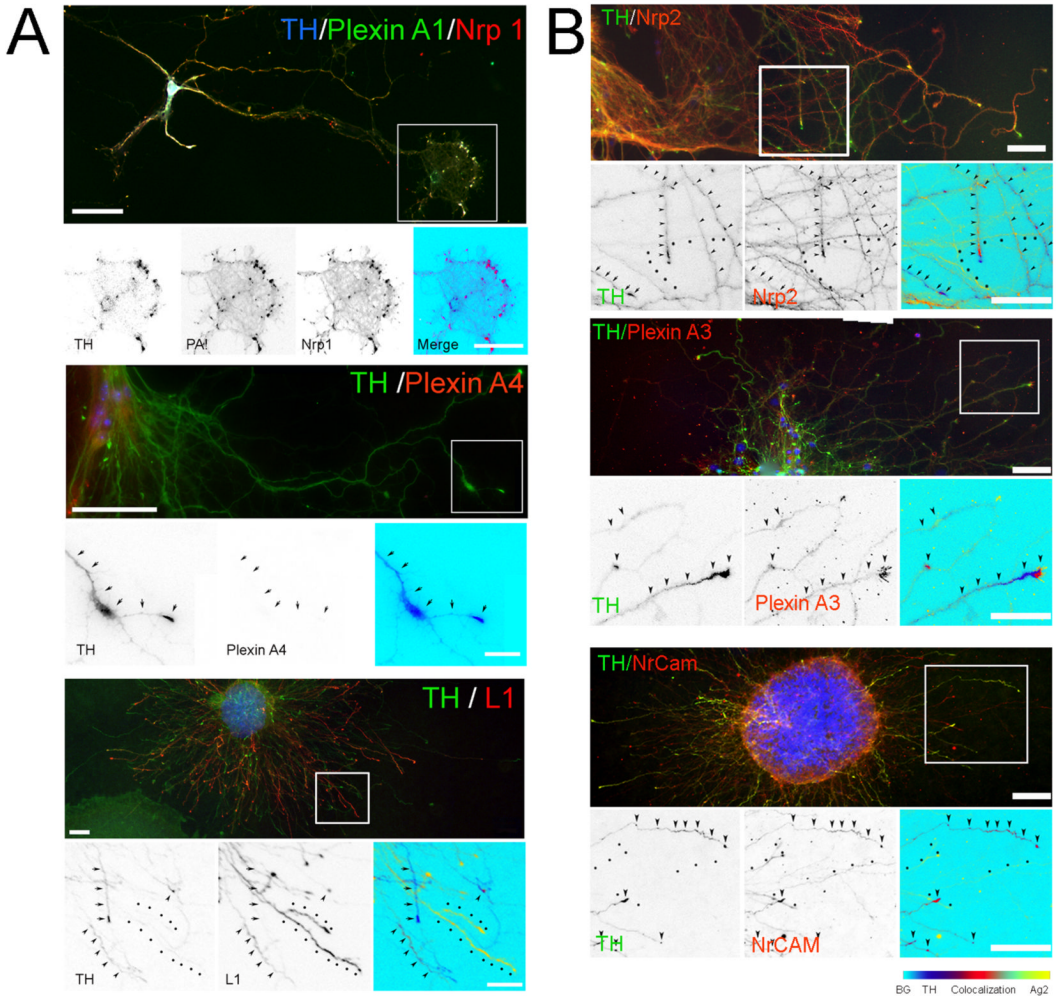

Figure 3. Expression of Sema3A and 3F receptors *in vitro*

Immunolocalization of the individual components of the Sema3A (A) and 3F (B) receptors in cultured E14 rat VM neurons is shown. VM neurons were cultured for 7 to 10 days and double-stained with antibodies against TH (green) and Nrp1, Nrp2, PlexinA1, PlexinA3, PlexinA4, L1 or NrCAM in red. Green and red signal co-localization is shown in the merge panel. Selected regions (white square) were enlarged to show the co-localization of the different receptor elements with TH-stained axons. In some cases merging was made as described in Fig. 2. Co-localization gradient bar is shown at the bottom right of the figure. Co-localization: arrowheads; TH: arrows, Second antigen: dots. Calibration bars: 50 μm.

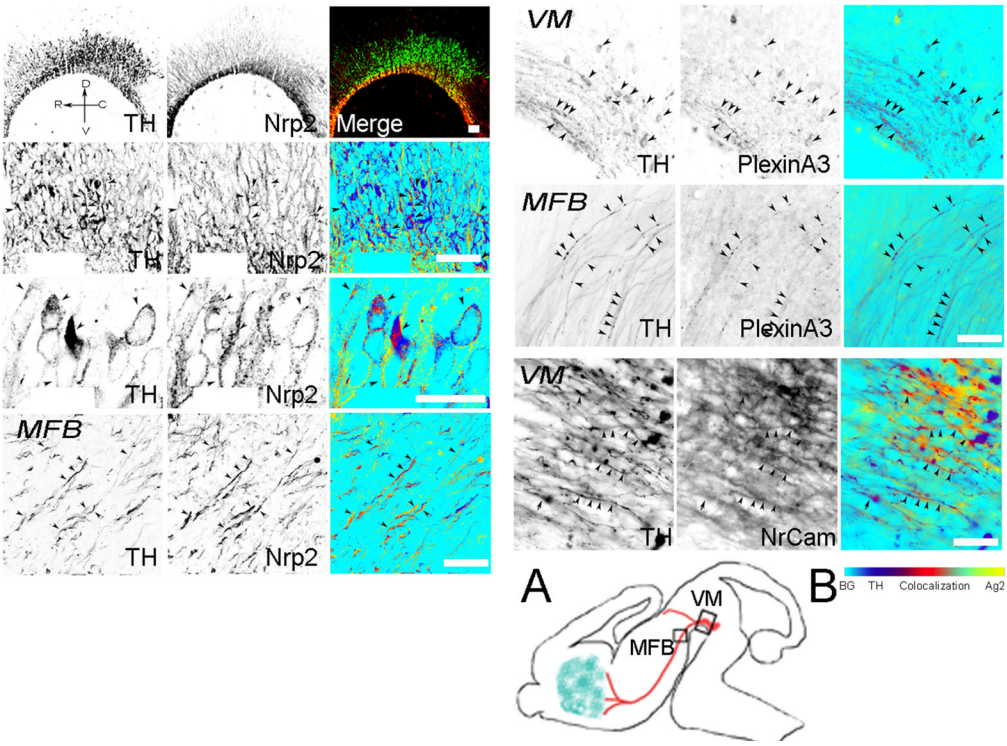

Figure 4. Expression of Sema3F receptors *in vivo*

The Sema3F receptor complex comprises Nrp2, PlexinA3 and NrCAM. The figure shows the immunolocalization of the individual components of the Sema3F receptor in the VM of E13.5 rat. Embryos were fixed and 20μm sagittal sections were cut within the region depicted in fig. 1, double-stained with antibodies against TH (green) and Nrp2, PlexinA3 or Nr-CAM (red). Green and red signal co-localization (arrowheads) is shown in the merge panel. In some cases merging was made as described in Fig. 2. (A) Diagram showing the regions where the VM or MFB pictures were taken. (B) Co-localization bar. Picture orientation is represented by the orientation cross in the top left panel. Calibration bars: 50 μm.VM, ventral mesencephalon; MFB, medial forebrain bundle.

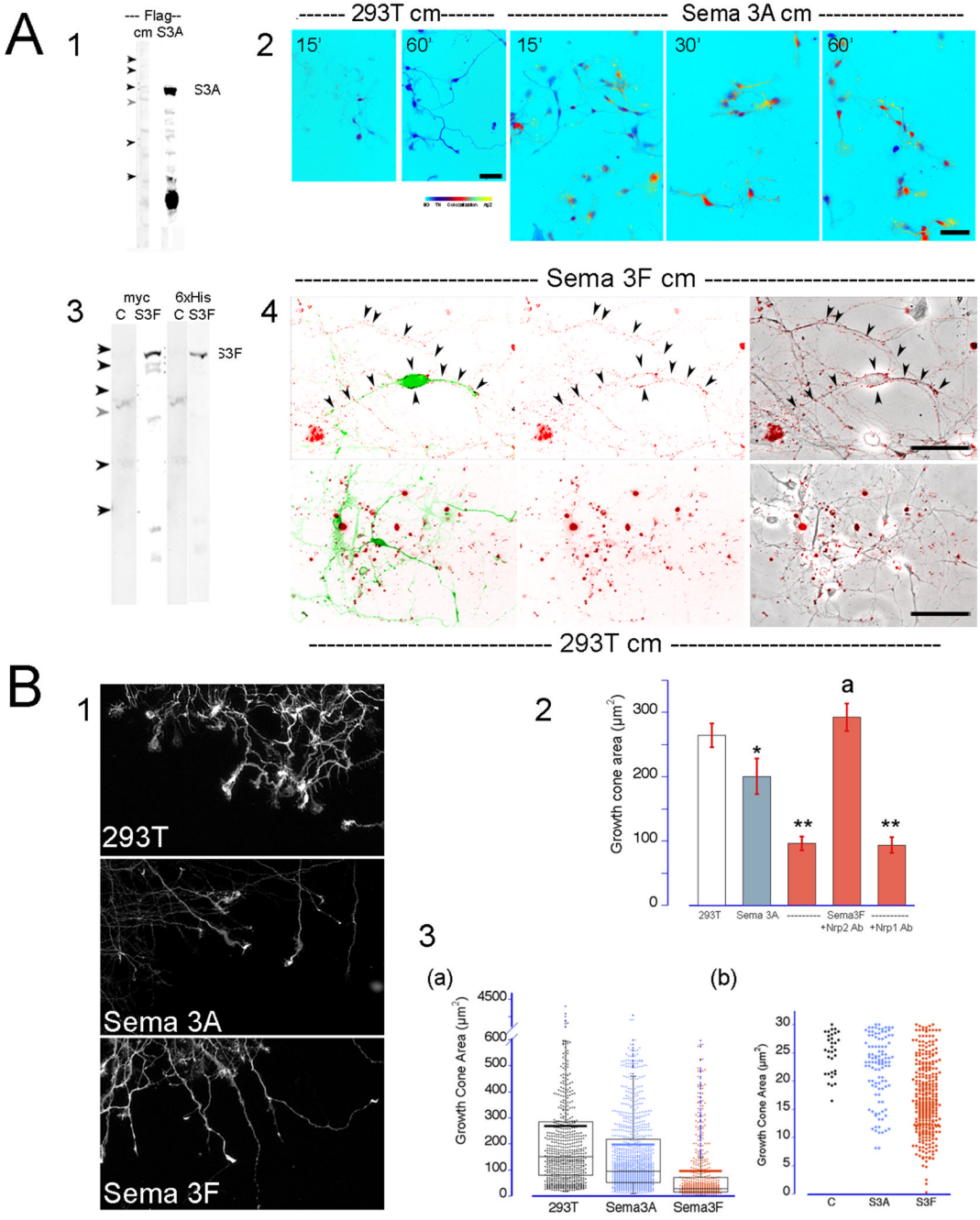

Figure 5. Sema3A and 3F bind to DA neurons and induce the collapse of growth cones

Dissociated cells or aggregates were treated with Sema3A, Sema3F or 293T (control) - conditioned media. (A) Semaphorin binding assays. Western blots with anti flag, 6×His or *myc* antibodies confirmed the presence of secreted Sema3A (1; S3A) or Sema3F (3; S3F) in conditioned media and their absence in control media (cm). (Arrowheads indicate the position for molecular weight markers, from top to bottom: 200, 150, 100, 75, 50 and 37 Kd). Media was preincubated with a monoclonal antibody directed against the *flag* (2) or *myc* (4) epitopes for 30 min at 37°C and then added to the cells for 15 to 60 minutes. Cells were fixed and double-stained for TH (green) and mouse IgGs (red). Sema3A bound to TH^+ and TH^- neurons. The label was weak and characterized by fine puncta in cell body and neurites. In contrast, Sema3F

bound largely to TH^+ neurons. Sema3F signal was found associated with the axon and the surface of the cell body (arrowheads). No surface staining of the neurons is visible following incubation of the cells with 293T-conditioned media. (B) Growth cone collapse assays. VM cell aggregates were cultured for 2-3 days and exposed to Sema3A, 3F or 293T conditioned media for 30 min. Cells were fixed and stained for TH. Pictures of the stained growth cones were taken at 40× magnification (1). The area of the TH^+ growth cones was measured in ImageJ (NIH). (2) The graph shows the effect of semaphorins on the vDA growth cone size. The bars represent the average growth cone surface area ± SEM from 7 to 9 independent cultures.*: $p \leq 0.03$. **: $p \leq 0.0001$ different from 293T. a: $p \leq 0.0001$ different from Sema3F (ANOVA followed by Student-Newman-Keul test). (3) Dot/box plot graph showing the distribution of the vDA growth cones areas in control and treated cultures (a). Thick horizontal bar represents the mean area of TH^+ growth cones. (b) Expanded view of small area vDA growth cones. Area of fully collapsed TH^+ growth cones ranged between 7 to 25 μm^2.

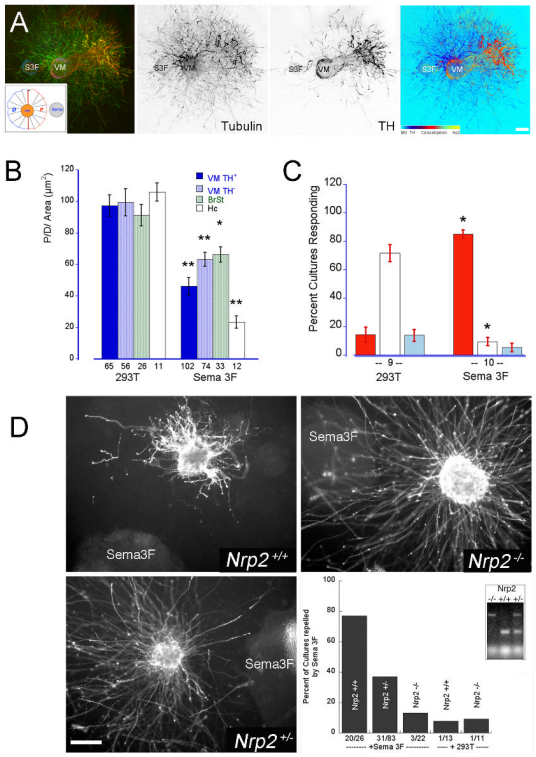

Figure 6. Sema3F is a strong repellent of DA axons

E14 VM rat explants were co-cultured with 293T-Sema3A producing cell aggregates for 2-3 days. Cultures were fixed and double-stained for TH (red) and tubulin (green) to distinguish DA axons. Untransfected 293T cell aggregates were used in control co-cultures. (A) The typical response elicited by Sema3F on VM explants. Note the strong repulsive effect of Sema3F on TH^+ axons in contrast to the weaker effect on TH^- axons. Inset: The effect of Sema3F was measured as the ratio between the proximal (P) and distal (D) hemiareas covered by axons with respect to the 293T cell aggregate. Calibration bar indicates 100 µm. (B) The graph represents the average P/D ratios ± SEM of ventro-mesencephalic (VM), brain stem (BrSt) or hippocampal (Hc) explants co-cultured with 293T or Sema3F aggregates. • $p<0.05$; •• $p< 0.005$ and ••• $p<0.0001$ when compared with controls (293T). (C) The P/D ratio of each co-culture was scored as repulsive when it was below -1SD from the 293T mean, as attractive when above +1SD, or un-responsive when it was within ± 1 SD. The bars represent the average percentage of cultures responding in one or another direction ± SEM. Note that more than 80% of the VM cultures analyzed were repelled by Sema3F. The number under the bars represents the number of independent cultures assayed. *: $p < 0.0001$ ANOVA followed by Student-Newman-Keul comparison test. (D) The repulsive effect of Sema3F on DA axons is lost in VM explants from *Nrp2$^{-/-}$ mice*. VM explants from wild type (*Nrp2$^{+/+}$*), heterozygous (*Nrp2$^{+/-}$*), and homozygous (*Nrp2$^{-/-}$*) mice were co-cultured with Sema3F-producing cell aggregates for 3 days, fixed and stained for TH. Cultures P/D ratios were measured and scored as repulsion when the P/D ratio was below 75. Calibration bar: 200 µm.

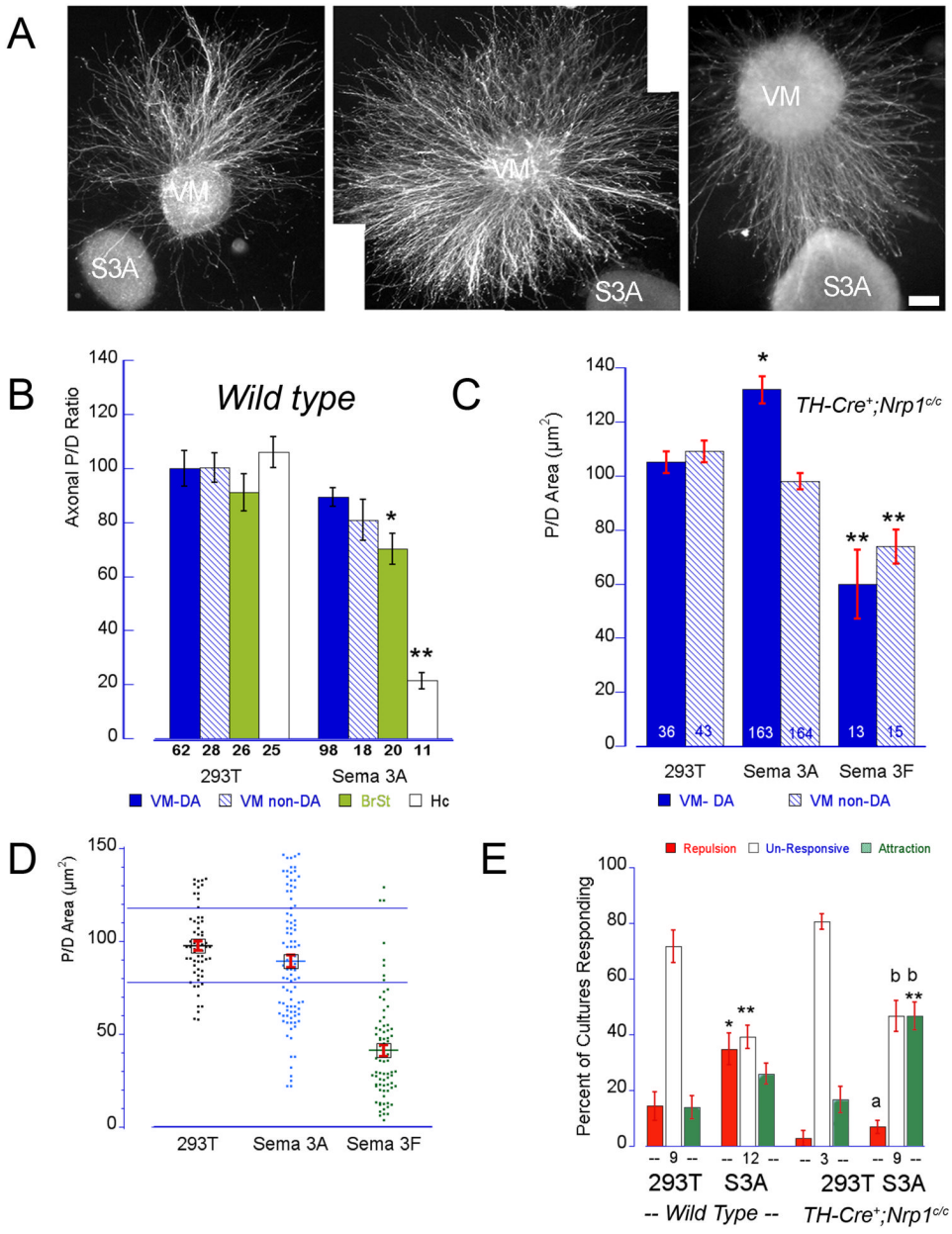

Figure 7. Sema3A repels a small population of DA axons

E14 VM rat explants were co-cultured with 293T-Sema3A producing cell aggregates for 2-3 days. Cultures were fixed and double-stained for TH (red) and tubulin (green) to distinguish DA axons. Untransfected 293T cell aggregates were used in control co-cultures. The response of TH^+ and TH^- axons was measured as P/D area ratio (see legend Figure 6). (A) TH-immunostained VM explants and the typical response elicited by Sema3A. Calibration bar indicates 100 μm. (B) Average P/D ratios ± SEM of VM, brain stem (BrSt) or hippocampal (Hc) axons co-cultured with 293T or Sema3A aggregates. Sema3A induced only a marginal effect on DA axons, being slightly more effective on non-DA axons from BrSt explants. As expected, Sema3A induced a very strong repulsive response on hippocampal (Hc) axons. (C)

Effect of Sema3A on vDA axons from *TH-Cre*$^{+}$;*Nrp1*$^{c/c}$ mice. The absence of Nrp1 accentuated the attractive response to Sema A but did not affect the Sema3F repulsive effect. • $p<0.05$; •• $p< 0.005$ and ••• $p<0.0001$ when compared with controls (293T). (D) Dot plot graph showing the P/D mean ± SEM as well as the distribution of the individual P/D ratios for each treatment. The blue horizontal lines represent ± 1 SD from the control mean. Note that while most of the Sema3F P/D ratios clustered below the -1 SD line, a large number of P/D ratios for Sema3A were above and below the SD lines. (E) Given the wide distribution of the Sema3A responses the P/D ratio of each co-culture was scored as repulsive when was below -1SD from the 293T mean, as attractive when above + 1SD, or unresponsive when it was within ± 1 SD. The bars represent the average percentage of cultures responding in one or another direction ± SEM. Note that more than ~36 % of the VM cultures analyzed were repelled by Sema3A. This effect was inhibited in explants from *TH-Cre*$^{+}$;*Nrp1*$^{c/c}$ mice while an increase in the percentage of cultures being attracted by Sema3A was detected. The number under the bars represents the number of independent cultures assayed. *: $p < 0.002$; **: $p <0.0001$ different from its wild type control; a: $p< 0.0002$; b: $p< 0.0005$ ANOVA followed by Student-Newman-Keul comparison test.

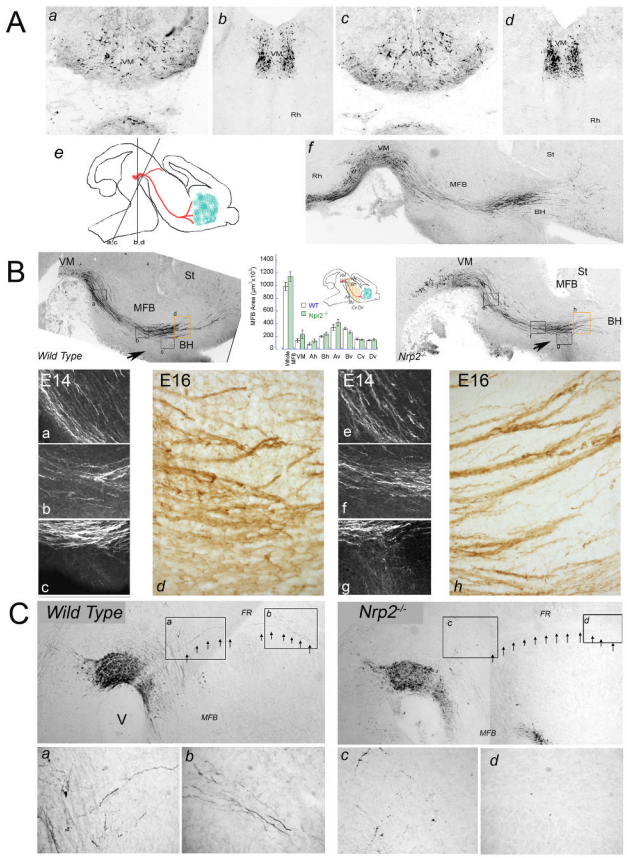

Figure 8. The meso-telencephalic DA pathway appears unaffected in *Nrp2*$^{-/-}$ mice

(A) 20 μm coronal sections from *wild type* (*a*,*b*) and *Nrp2*$^{-/-}$ mouse E16 embryos (*c*,*d*) were cut at different angles (*e*) to better visualize the aberrant growth of DA neurites. Most *Nrp2*$^{-/-}$ brains showed a normal TH^{+} fiber and cell organization in the VM. Only one *Nrp2*$^{-/-}$ mouse out of 16 (*f*) showed TH^{+} cells and axons extending caudally into the rhombencephalon (compare with B). (B) Twenty micron parasagittal tissue sections were cut from E12-16 wild type and *Nrp2*$^{-/-}$ mouse embryos as depicted in Fig. 1 and stained for TH. The number and organization of the *Nrp2*$^{-/-}$ VM DA neurons were undistinguishable from wild type. TH^{+} fibers running along the MFB have similar ventro-dorsal organization in E16 wild type and *Nrp2*$^{-/-}$ mouse brains. The area occupied by the MFB was measured in 3 to 5 parasagittal sections from 3 wild type and mutant mice. The graph shows the area of the whole MFB measured from the rostral end of the mesencephalic flexure to the internal capsule. The area occupied by the MFB was also measured in 500 μm wide segments distributed in 3 rows (VM, Ah, Bh) and 4 columns (Av-Dv) along the track. Although the MFB of *Nrp2*$^{-/-}$ embryos seems to spread dorsally no significant differences were found with the *wild type*. High magnification of the areas framed in the upper panels show detail of TH^{+} axons running along the MFB in E14 (*a*,*b*,*c*) and E16 (*d*,*e*) brains. Note that the degree of fasciculation of the TH^{+} axons is similar in both wild type and *Nrp2*$^{-/-}$ brains. Arrows indicate TH^{+} axons entering the basal hypothalamus (BH). (C) The DA mesohabenular pathway running along the fasciculus retroflexus (FR, arrows) was severely disturbed by the *Nrp2*$^{-/-}$ mutation. (*ad*): High magnification of the areas framed in the upper panels showing TH^{+} fibers running along the FR. Note the virtual disappearance of these fibers in the *Nrp2*$^{-/-}$ mouse.

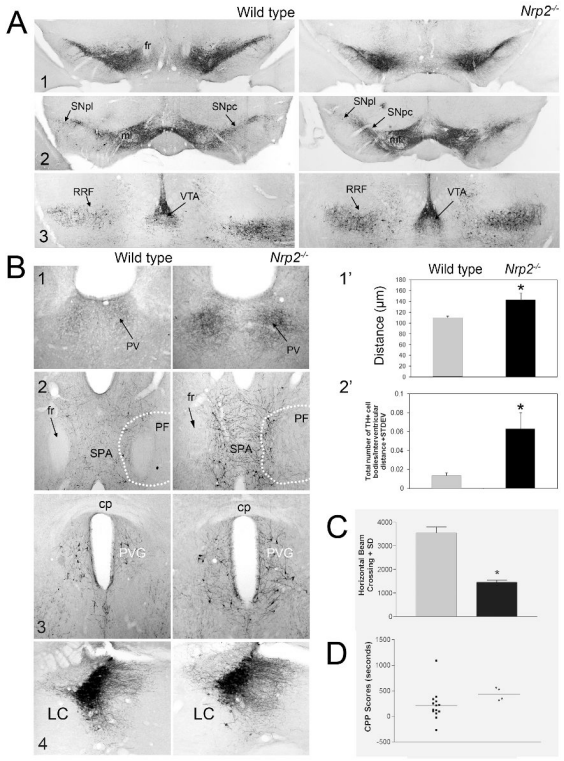

Figure 9. Anatomical phenotype and behavioral correlate of adult *Nrp2*$^{-/-}$ mice

Coronal 20 μm slices were cut from adult wild type and *Nrp2*$^{-/-}$ mice and stained for TH. (A) Organization of TH^{+} cells at different planes through the VM is shown (1-3: rostral to caudal). The number and organization of the *Nrp2*$^{-/-}$ VM DA neurons was indistinguishable from wild type. (B) TH^{+} non-DA cells and fibers become disturbed in the *Nrp2*$^{-/-}$ mouse. (1) Cells and fibers in the paraventricular nucleus of the thalamus (PV) become more densely stained and lateralized. The graph in (1′) shows the distance between the edges of this bilateral nucleus measured after thresholding sections from at least 3 different animals. (2) TH^{+} non-DA cells and fibers in the medial region of the nucleus parafascicularis (PF) and subparafascicular area (SPA). The graph in (2′) shows the average number of TH^{+} cells ± SEM counted in the SPA of at least 3 wild type and *Nrp2*$^{-/-}$ mice. *: $p < 0.05$. This pattern continues more caudally (3) and in the periventricular gray area (PVG) the number of cells is also elevated but no significant differences were found in the locus coeruleus (LC; 4). (C) The basic components of motor behavior were measured in wild type and *Nrp2*$^{-/-}$ mice (see Methods). Average locomotor activity ± SEM was significantly decreased in *Nrp2*$^{-/-}$ mice. (D) We also used a biased conditioned place preference test to evaluate the *Nrp2*$^{-/-}$ mutant mice, but no significant differences were observed. Other abbreviations: ml, medial lemniscus; SNc, substantia nigra pars compacta; SNl, substantia nigra pars lateralis; RRF, retrorubral field; VTA, ventral tegmental area.